JOURNAL OF PETROLOGY | VOLUME 43 | NUMBER 7 | PAGES 1259–1286 | 2002

A Bimodal Alkalic Shield Volcano on Skiff Bank: its Place in the Evolution of the Kerguelen Plateau

BRUNO KIEFFER[1,2], NICHOLAS T. ARNDT[1]* AND DOMINIQUE WEIS[2]

[1]LABORATOIRE DE GÉODYNAMIQUE DES CHAÎNES ALPINES, OSUG, UMR 5025 CNRS, BP 53, 38041 GRENOBLE, FRANCE
[2]DÉPARTEMENT DES SCIENCES DE LA TERRE ET DE L'ENVIRONNEMENT, UNIVERSITÉ LIBRE DE BRUXELLES 50, AV. F. D. ROOSEVELT, B-1050, BRUSSELS, BELGIUM

RECEIVED JULY 10, 2001; REVISED TYPESCRIPT ACCEPTED JANUARY 31, 2002

A bimodal volcanic sequence of 230 m thickness on Skiff Bank, a western salient of the northern Kerguelen Plateau, was drilled during ODP Leg 183. The sequence comprises three main units: a mafic unit of trachybasalt flows sandwiched between two units of trachytic or rhyolitic flows and volcaniclastic rocks. Although interpretation is complicated by moderate to strong alteration of the rocks, their original chemical character can be established using the least mobile major and trace elements (Al, Th, high field strength elements and rare earth elements). High concentrations of alkalis and incompatible trace elements indicate that both mafic and felsic rocks are alkalic. The felsic rocks may have been derived by partial melting of mafic rocks, followed by fractionation of feldspar, clinopyroxene, Fe–Ti oxides and apatite. The mafic and felsic rocks have similar Nd and Pb isotopic compositions; $^{206}Pb/^{204}Pb$ ratios are low (17·5–18·0) but, like the $^{143}Nd/^{144}Nd$ ratios (0·5125–0·5126), they are comparable with those of basalts from the central and southern Kerguelen Plateau (e.g. Sites 747, 749, 750). The Sr isotopic system is perturbed by later alteration. There is no chemical or isotopic evidence for a continental crustal component. The bimodal alkalic character and the presence of quartz-phyric rhyolites is interpreted to indicate that the sequence forms part of a shield volcano built upon the volcanic plateau. The age of 68 Ma, obtained on Site 1139 rocks by Duncan (A time frame for construction of the Kerguelen Plateau and Broken Ridge, Journal of Petrology **43**, *1109–1119, 2002), provides only a minimum age for the underlying flood volcanic rocks. The high age indicates none the less that Skiff Bank is not the present location of the Kerguelen plume.*

KEY WORDS: *Ocean Drilling Program; Kerguelen Plateau; Skiff Bank*

INTRODUCTION

The Kerguelen Plateau was for many years been considered, along with Ontong Java, as a type example of an oceanic plateau. This plateau, a pile of mafic rocks of 20–30 km thickness, covers an area of $\sim 2 \times 10^6$ km^2 (three times the size of France) in the southern Indian Ocean. Like Ontong Java, it was thought to have formed through massive basaltic volcanism, which erupted in an entirely oceanic setting as a large mantle plume impinged on the base of the oceanic lithosphere. As explained in recent papers (Frey *et al.*, 2000*a*; Weis *et al.*, 2001; Ingle *et al.*, 2002), two discoveries have changed these ideas. The first was the demonstration by Mahoney *et al.* (1995) that basalts from the southern part of the plateau have geochemical and isotopic compositions that indicate that they had interacted with continental lithosphere. The second was the recovery, at several sites of Leg 183 of the Ocean Drilling Program (ODP), of volcanic and sedimentary sequences whose geological and geochemical characteristics provided clear evidence of emplacement near continental crust. Because of these discoveries, Kerguelen is now thought of as a hybrid plateau, with an older southern portion made up, at least in part, of volcanic rocks resembling submerged continental flood basalts, and a younger northern portion that erupted in a purely oceanic setting (Frey *et al.*, 2000*a*).

Skiff Bank (or Leclaire Rise), is the northwestward extension of the Kerguelen Plateau (Fig. 1). It was sampled by drilling during ODP Leg 183. The site, one

*Corresponding author. Present address: Laboratoire de Géodynamique des Chaînes Alpines, OSUG, UMR 5025 CNRS, BP 53, 38041 Grenoble, France. E-mail: arndt@ujf-grenoble.fr

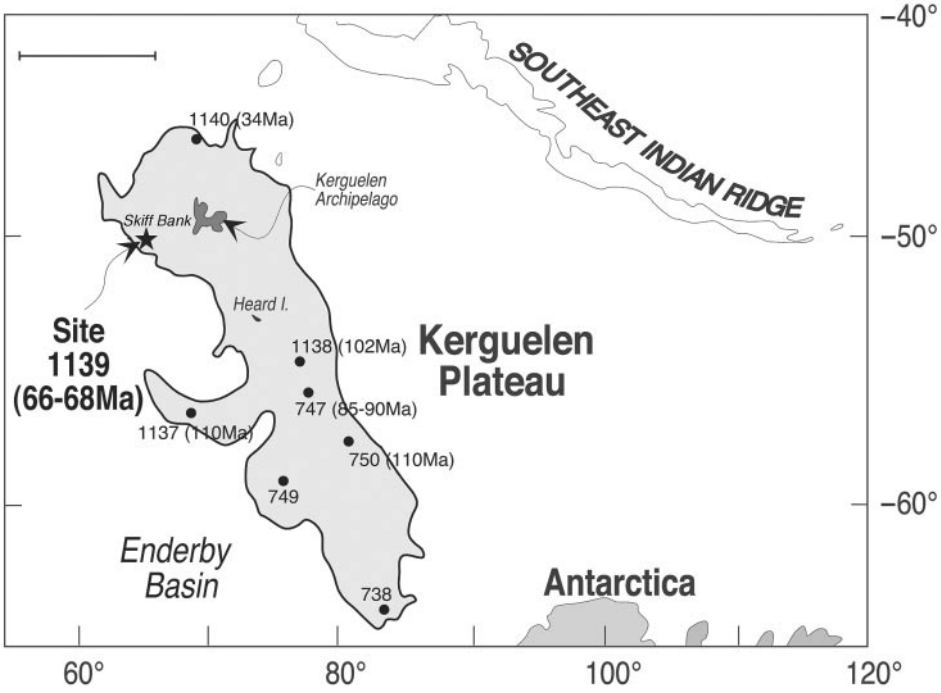

Fig. 1. Bathymetric map of the Kerguelen Plateau. Contour is the 3 km isobath. Sites 738, 747, 749 and 750 were drilled during ODP Leg 120 and Sites 1137, 1138, 1139 and 1140 were sampled during Leg 183.

of six that reached volcanic basement, was selected for two main reasons:

(1) one goal was to provide some information about the age and the character of the volcanic rocks in the northern part of the plateau. Before Leg 183, the only available samples from the northern part of the Kerguelen Plateau were from a suite of trachybasaltic lavas, microgabbros, alkali granites and sedimentary rocks recovered by dredging during the Kerimis cruise (Schlich *et al.*, 1998; Weis *et al.*, 2002). Given the generally felsic character and the diversity of rock types in this assemblage, these rocks were interpreted as probable ice-rafted debris and not the predominant rocks of this part of the Kerguelen Plateau. The closest drill site that penetrated basement was 747 of Leg 120, which is situated in the southern part of the central plateau. As indicated in Fig. 1, Sites 1139 and 1140 were the two Leg 183 sites selected to document the characteristics of the northern part of the plateau.

(2) Knowledge of the age and the volcanic and tectonic environment of this part of the Kerguelen Plateau is crucial to our understanding of the overall evolution of the plateau. A key issue stems from the proposition of Duncan & Storey (1992) and Müller *et al.* (1993) that Skiff Bank is the current site of the Kerguelen plume. If this were true, the volcanic sequence at the site would include rocks that are much younger than those of the main plateau, with distinctive petrological characteristics. It is important to track the position of the plume if we are to understand the interaction between magmatic and tectonic events that led to the evolution of the plateau.

The drilling at Site 1139 passed through 460 m of sediments, then penetrated a sequence of lavas and volcaniclastic rocks of 230 m thickness. Two unexpected results emerged immediately from shipboard study of the volcanic drill core (Shipboard Scientific Party, 2000). First, the volcanic rocks have bimodal mafic–felsic compositions with a strongly alkalic magmatic character; as such, they are very different from the monotonous tholeiitic flood basalts of normal oceanic plateaux. Second, the Eocene to Oligocene age (33–34 Ma) of the sediments that immediately overlie the volcanic sequence provides a relatively high minimum age for the underlying volcanic rocks. The volcanic rocks cannot, therefore, represent the products of recent plume-related magmatism. However, this minimum age is also significantly less than the ~90 Ma age inferred from available radiometric and stratigraphic dating for the central part of the plateau. The results suggested that the volcanic sequence at Site 1139 is distinct from those of both the main plateau and from younger plume-related activity, such as that on the Kerguelen Archipelago and on Heard and Macdonald Islands.

In this paper we present the results of a detailed petrological and geochemical investigation of samples from Site 1139. Our study included inductively coupled

plasma mass spectrometry (ICP-MS) analyses of a wide suite of trace elements and determination of the Nd, Sr and Pb isotopic compositions of the volcanic rocks. Our new results, combined with new age dates of Duncan & Pringle (2000) and Duncan (2002) and comparisons with bimodal volcanic series from two other areas, allow us to clarify (1) the volcanic and tectonic setting of Skiff Bank, (2) the relationship between this region and the rest of the northern plateau, and (3) the magmatic evolution of the Kerguelen Plateau as a whole.

Geological setting

Skiff Bank is the westernmost salient of the northern Kerguelen Plateau and lies ~350 km WSW of the Kerguelen Archipelago (Fig. 1). It is a broad, relatively flat bank, about 300 km long and 150 km wide; the minimum water depth on the central ridge is ~200 m, increasing to ~3500 m at the margins. The bank is elongated in an east–west direction, sub-perpendicular to fractures in the surrounding Enderby Basin but parallel to the direction of rifting between the Indian and Antarctic continents. The southern border of the Bank is marked by a large negative gravity anomaly, a feature absent from the northern border (Sandwell & Smith, 1997; Shipboard Scientific Party, 2000). In seismic profiles (Recq & Charvis, 1986; Recq *et al.*, 1990, 1994; Charvis *et al.* 1995), the structure of the northern plateau is relatively simple. A thin sedimentary section (400–500 m) overlies an igneous basement of 14–19 km thickness.

Site 1139 is located at 50·18°S and 63·94°E, ~50 km south of the central ridge at a water depth of 1427 m, and is on the flank of one of two broad edifices at the surface of the plateau (Shipboard Scientific Party, 2000, fig. F32). The maximum age of the overlying sediments was established as early Oligocene to latest Eocene (Shipboard Scientific Party, 2000).

Felsic volcanic rocks from Site 1139 were dated by Duncan & Pringle (2000) and Duncan (2002) using the Ar–Ar method. Incremental heating experiments on both whole rocks and on feldspars separated from rhyolites and trachytes yielded ages of 66–68 Ma. These ages are ~35 Myr greater than the 33–34 Ma age assigned to the earliest Oligocene to latest Eocene sedimentary rocks that directly overlie the volcanic units at the Site (Shipboard Scientific Party, 2000).

Petrography and mineralogy of the volcanic rocks of Site 1139

The 230 m basement sequence at Site 1139 is composed of bimodal mafic–felsic volcanic rocks with rare intercalated terrigenous and volcanogenic sediments. Detailed descriptions of the petrological characteristics of these rocks, as determined through study of the drill core, are given in the report of the Shipboard Scientific Party (2000) and will not be repeated here. Instead we show in Fig. 2 a log of the main units. We summarize the main petrological features in the following paragraphs, using a combination of shipboard observations and our own petrographic investigations.

As shown in Fig. 2, a 73 m series of trachybasaltic lava flows is sandwiched between two series of felsic volcanic rocks. The upper 125 m felsic series contains both rhyolitic and trachytic lava flows and volcanoclastic rocks; the lower 32 m series is made up of two trachytic lava flows. Core recovery was poor, ~21%, in the upper felsic sequence, probably because of the presence of numerous rubbly breccia zones, but better in the more massive mafic and lower felsic sequences (61% and 68%). Interpretation of volcanic structures and textures led the Shipboard Scientific Party (2000) to conclude that the rocks erupted subaerially.

Five units were recognized in the upper felsic sequence. Unit 1 consists of rhyolite rubble and breccia, with thin interbedded layers of bioclastic sandstone and volcaniclastic sediments. Most of the rock is sparsely phyric to glassy, in one case with perlitic textures. Phenocrysts are sparse, mainly sanidine with rare quartz. Haematite in the groundmass imparts a reddish brown colour to the rocks. The perlitic glass in the basal breccia appears silicified and contains a small amount of chalcedony. The vesicle content of this unit is very low, <2%.

Unit 2 is a dark red (oxidized) rhyolite containing ~10% sanidine and minor quartz phenocrysts. Flattening and agglutination of fragments suggest that this unit is a welded pyroclastic flow. Many of the quartz and sanidine phenocrysts are shattered. No ferromagnesian minerals are present, but clays and oxides are abundant and could be the products of the alteration of mafic phases. The unit contains <2% vesicles.

Unit 3 is strikingly different from the overlying units. It consists of a green-coloured, highly altered crystal-vitric tuff containing abundant sanidine (15%) and rarer quartz phenocrysts and lithic clasts in a perlitic, and locally banded glassy matrix. This unit is interpreted as the densely welded core of a pyroclastic flow deposit. The green colour arises from intense alteration of the matrix glass.

Unit 4 is a massive to brecciated, vesicular, dark red (oxidized) rhyolite similar to Unit 2. Here again the quartz and sanidine phenocrysts are shattered and some show embayments at their margins. Goethite is abundant in the groundmass cement.

Unit 5 consists of a central zone of massive, highly altered trachytic lava bounded at both margins by brecciated zones. This unit is interpreted as a differentiated lava flow. Phenocryst phases are sanidine, and ferromagnesian minerals that are completely replaced by

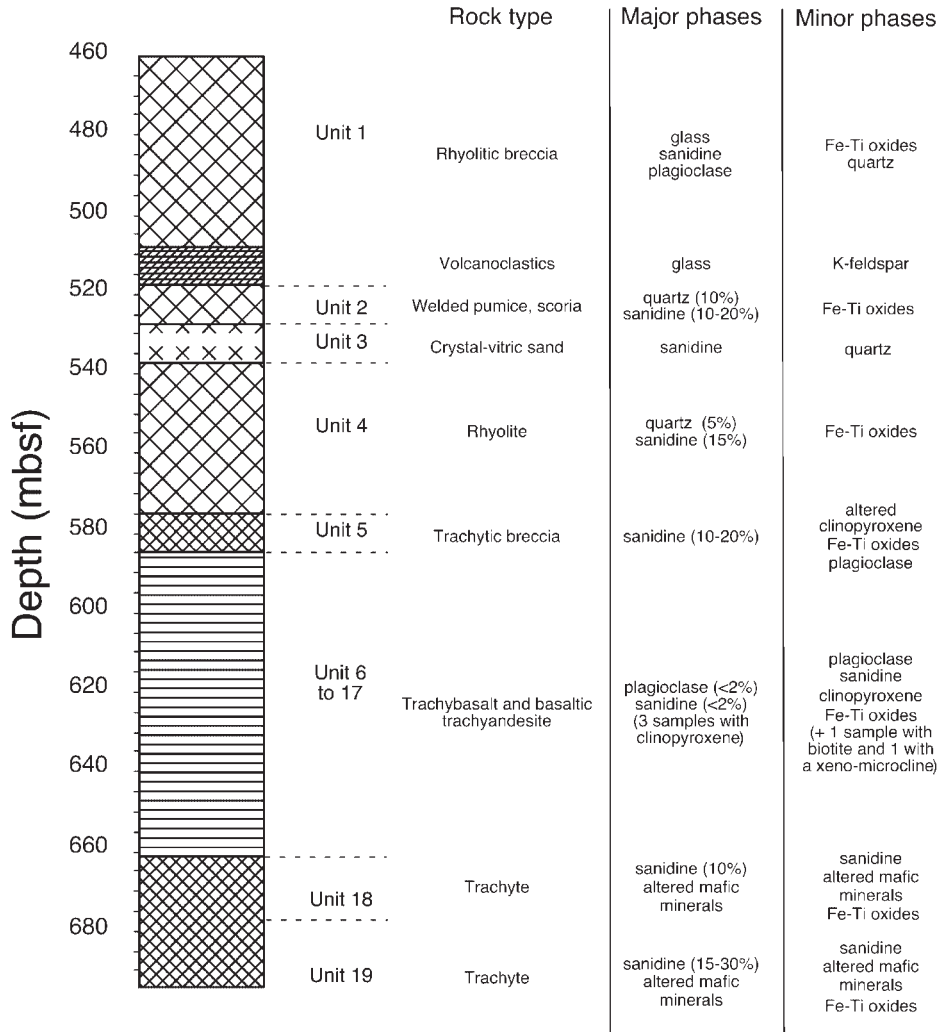

Fig. 2. Simplified log of the volcanic sequence with petrographic descriptions and rock types.

secondary chlorite, carbonate and clays. The same minerals fill fissures and vesicles (<5%).

The middle sequence, Units 6–17, comprises 12 flows or flow units with mafic to intermediate compositions. These units, whose thickness varies from 2 to almost 20 m, have massive interiors overlain by thin flow-top breccias. Unit 10 consists of small pahoehoe lobes, Unit 11 is an aa flow, and the other units have brecciated margins of indeterminate character. These features indicate subaerial emplacement. These units contain between 0 and 20% of vesicles filled with secondary minerals (clays, zeolite, carbonate and chlorite).

The lava has a pale grey colour and contains 1–3% plagioclase and sanidine phenocrysts in a fine-grained, trachytic-textured groundmass. The least altered samples contain 1–2% of unaltered phenocrysts of pale brown, Ti-rich clinopyroxene in a matrix of feldspar, abundant opaque minerals and patches of secondary minerals (clay minerals and carbonate) that could represent altered clinopyroxene. Some of the feldspar crystals have the form and habit of primary magmatic sanidine; others could represent altered plagioclase. The more altered samples contain feldspar phenocrysts in a matrix completely altered to secondary minerals. The most common alteration minerals are siderite, calcite, chlorite, sepiolite, and secondary Fe oxides. Patches of Fe oxides and clay minerals could represent completely altered ferromagnesian minerals.

The lower felsic sequence, Units 18 and 19, consists of an almost complete section through one lava flow (Unit 18) and the upper part of a second flow (Unit 19). Both units were originally composed of porphyritic trachyte containing 10–30% clinopyroxene and sanidine phenocrysts in a fine-grained, poorly vesicular matrix. Subsequent moderate to intense alteration has destroyed most of the primary minerals. Clay minerals or siderite has

replaced all the clinopyroxene, and rare titanomagnetite phenocrysts are altered to maghemite or haematite. The groundmass is composed of alkali feldspar (some of which may be altered plagioclase), quartz, magnetite and altered glass. Secondary phases in the matrix include clay minerals, abundant siderite, haematite and chalcedony.

ANALYTICAL METHODS

The samples were ground in an agate mortar. Major elements and certain trace elements (Ni, Cr and V) were analysed by X-ray fluorescence (XRF) at the University of Massachusetts, Amherst (Rhodes, 1983). Other trace elements were analysed by ICP-MS at the University of Grenoble following the procedure of Barrat *et al.* (1996, 2000). The error on major element determinations is <5%. For the trace elements Rb, Sr, Ba, Hf, Zr, Ta, Nb, U, Th, Pb, Y and rare earth elements (REE), the accuracy is better than 5%; for Cs it is ~10%. Table 1 contains the major and trace element data, along with measurements of standards BIR1, BHVO and RGM. The results are in excellent agreement with the data of Eggins *et al.* (1997). The data that are reported in Table 1 and plotted in the figures were recalculated on a volatile-free basis.

Nd, Sr and Pb isotopic analyses were carried out at Université Libre de Bruxelles on a VG 54 mass spectrometer using the procedure described by Weis *et al.* (1987). All samples were leached in 6N HCl in an ultrasonic bath to remove secondary minerals and seawater following the procedure described by Weis & Frey (1991). Each leaching period was 20 min and the procedure was repeated 10 or more times, until a clear solution was obtained. The average total weight loss during leaching varied between 21 and 64%. No correlation between loss on ignition (LOI) and weight loss was evident and there was no difference between mafic and felsic rocks. To evaluate the effects of leaching, two duplicate analyses were also run on unleached samples. Sr isotopic ratios were normalized to $^{86}Sr/^{88}Sr = 0{\cdot}1194$ and Nd isotopic data were normalized using $^{146}Nd/^{144}Nd = 0{\cdot}7219$. The average $^{87}Sr/^{86}Sr$ value for NBS 987 Sr standard was $0{\cdot}710278 \pm 12$ ($2\sigma_m$ on the basis of 12 samples). Analyses of the Rennes Nd standard yielded $^{143}Nd/^{144}Nd = 0{\cdot}511970 \pm 7$ ($2\sigma_m$ on the basis of 12 samples). Pb isotopic ratios were measured on single Re filament using the H_3PO_4–silica gel technique. All Pb isotopic compositions were corrected for mass fractionation ($0{\cdot}12 \pm 0{\cdot}04\%$ per a.m.u.) based on 10 analyses of NBS 981 Pb standard run at a temperature between 1090 and 1200°C.

Influence of alteration on chemical compositions

Interpretation of the chemical compositions of Site 1139 rocks is greatly complicated by the moderate to intense alteration that has affected all samples. As is discussed in a later section, this alteration has had major effects on the compositions of the lavas, but these effects are different in the mafic and felsic rocks. Particularly in the felsic lavas, the crystallization of feldspar and minor phases complicates the distinction between mobile and immobile behaviour. The removal of these minerals drastically changes the concentrations and ratios of elements such as Ti, P, Eu, Sr and Ba. Furthermore, the peculiar and intense nature of the alteration appears to have changed the concentrations of some elements that are normally considered to be immobile.

Some examples of complex behaviour of minor and trace elements in the felsic lavas are illustrated in the variation diagrams plotted as Fig. 3. Zirconium correlates well with Nb, an element normally considered immobile, but poorly with Ti, another high field strength element (HFSE) that is also thought to resist alteration. The scatter in the Zr vs Ti diagram probably is not due to mobility of Ti but to variable amounts of oxide fractionation. The REE, with the exception of Eu and Ce, are also thought to be relatively immobile. However, two representative REE, La and Yb, show almost as much scatter as Ba and Rb, elements that are regarded as moderately to highly mobile. The mafic lavas plot as a tight group in most trace element diagrams, as shown in a subsequent section, but we will demonstrate later that their major element compositions may have been strongly affected by alteration.

In view of these complications, it is not possible to define, in general terms, which elements are mobile and which elements are not. For this reason we have chosen first to present the geochemical data, making reference where appropriate to the possible influences of alteration. Then, in the discussion section, we consider how the alteration has influenced the compositions of both the mafic and felsic lavas and establish which elements can be used to infer the magmatic histories of the two rock suites.

Major and trace elements

In the total alkalis–silica diagram (Le Bas *et al.*, 1986; Fig. 4), the mafic rocks plot in the fields of trachybasalt, basaltic trachyandesite, tephrite or phonotephrite. To avoid these rather cumbersome names we will refer to these rocks simply as trachybasalts. The felsic lavas show a wide range of compositions extending from trachyte well into the field of rhyolite. All these rocks plot in the alkalic domain, above the line that separates tholeiitic

Table 1: Major and trace element data

Sample:	51R1	52R1	52R1	52R1	53R1	53R2	54R1	55R1	55R1	56R3	57R1	59R1	61R1	61R1	61R2	62R2	62R2	63R1
	13–19	2–7	45–50	130–139	89–93	67–75	1–9	67–72	67–72	101–107	127–134	68–73	67–73	131–138	93–97	74–79	113–120	10–18
Unit:	1	1	1	1	1	1	1	2	2	3	4	4	5	5	5	6	6	6
Rock type:	R	R	R	R	R	R	R	R	Dup.	D	R	R	Tr	Tr	Tr	BTA	BTA	Te
Depth (mbsf):	475	480	490	495	500	505	509	518		531	540	560	575	580	582	585	586	595
SiO_2	72·4	76·1	76·1	72·5	74·4	74·8	75·5	77·3		68·4	77·9	80·4	66·4	67·2	67·1	53·0	50·6	47·9
TiO_2	0·32	0·34	0·33	0·32	0·34	1·15	0·32	0·31		0·47	0·28	0·27	0·50	0·51	0·50	3·17	3·16	4·35
Al_2O_3	12·6	10·9	10·7	10·9	10·4	10·8	10·5	10·7		15·8	9·5	9·2	15·7	15·6	15·7	19·0	18·8	16·6
Fe_2O_3	4·31	3·49	3·52	4·87	5·80	4·62	4·70	3·02		5·31	4·27	2·59	5·63	5·05	5·50	12·4	15·9	14·4
MnO	0·04	0·01	0·02	0·04	0·13	0·06	0·02	0·01		0·02	0·01	0·01	0·30	0·28	0·07	0·08	0·13	0·60
MgO	0·03	0·03	0·06	0·25	0·80	0·34	0·07	—		3·73	—	—	0·06	0·05	0·07	0·80	1·16	1·67
CaO	0·07	0·05	0·09	0·10	0·40	0·40	0·04	0·03		0·42	0·02	0·02	0·29	0·28	0·26	2·19	2·28	5·17
Na_2O	4·43	3·72	3·63	1·74	2·67	2·01	3·08	3·52		3·14	3·04	2·77	4·86	4·55	4·03	3·08	2·60	4·05
K_2O	5·36	5·21	5·13	8·94	4·29	5·05	5·23	4·73		2·12	4·48	4·59	5·87	5·97	6·05	4·31	4·02	3·07
P_2O_5	0·02	0·02	0·06	0·03	0·02	0·04	0·02	0·02		0·18	0·01	0·01	0·02	0·02	0·02	1·33	1·37	1·62
Total	99·6	99·9	99·6	99·7	99·3	99·3	99·4	99·7		99·6	99·5	99·9	99·7	99·5	99·3	99·3	100·0	99·5
LOI	0·80	0·46	0·85	3·11	10·4	8·08	0·97	0·75		14·6	0·80	0·72	2·69	2·35	1·68	6·98	9·74	6·69
Rb	151	203	159	162	96·4	127	194	111	112	37·5	117	115	81·4	94·0	118	60·2	59·2	47·9
Cs	0·39	0·99	0·49	0·44	5·26	1·13	0·68	0·21	0·21	1·19	0·22	0·18	0·17	0·36	1·68	0·86	0·98	0·21
Sr	5·74	7·71	14·2	16·3	66·8	50·3	6·62	4·13	4·34	48·20	3·26	3·65	7·25	6·58	9·12	136	149	491
Ba	4·95	5·08	5·57	10·9	34·5	102·1	4·63	19·8	18·7	7·42	10·6	15·6	30·2	29·9	33·9	852	950	1158
Hf	34·5	32·7	34·3	46·4	42·6	32·6	42·0	17·9	18·5	39·0	20·5	21·4	13·9	15·5	15·8	9·39	9·63	7·22
Zr	1750	1696	1475	2105	2015	1519	1814	857	862	1787	912	949	625	718	748	414	447	348
Ta	8·98	8·64	8·50	12·3	11·5	8·56	10·6	4·70	4·87	10·54	5·35	5·32	4·16	4·73	5·01	2·94	3·15	2·50
Nb	177	150	147	205	193	165	199	80	82·4	190	97·9	91·3	75·8	87·4	93·0	47·7	56·9	43·8
U	2·41	1·80	2·00	2·64	4·58	10·76	4·21	1·11	1·15	2·86	1·94	4·12	2·30	2·90	3·81	0·75	0·89	0·78
Th	18·7	18·0	19·5	26·4	23·7	17·7	25·2	10·2	10·3	22·9	11·7	12·4	9·8	10·7	11·1	4·16	4·39	3·16
Pb	11·4	5·6	10·3	22·3	30·9	25·6	18·8	14·5	11·7	32·7	17·3	17·0	12·4	10·3	14·5	6·90	6·69	5·01
Y	159	141	138	123	144	145	175	36·5	36·4	95·2	48·4	40·0	53·1	66·4	71·8	50·0	56·5	48·7
Ni		4·02		3·10	1·12	2·18		—		1·17	—	—	—	—	—	—	—	—
Cr		2·01		5·16	7·82	9·80		1·01		28·11	1·01	—	2·06	—	1·02	3·23	5·54	0
V		29·1		3·10	—	32·7		4·03		—	—	1·01	—	1·02	—	112	104·1	240
La	53·7	32·1	230	195	180	152	32·8	37·6	38·0	170	46·9	53·0	62·6	75·5	88·7	53·1	65·3	53·6
Ce	58·7	149	208	393	337	296	85·0	173	173	323	131	203	129	150	181	110	132	112
Pr	15·3	9·9	57·4	44·6	42·0	35·2	9·2	11·0	11·1	42·9	12·2	13·7	15·4	17·9	21·0	14·3	16·5	14·2
Nd	62·9	37·1	203	164	156	132	39·5	42·8	42·9	159	48·3	50·5	59·3	67·9	78·2	59·8	68·5	60·3
Sm	19·2	11·2	34·0	32·2	30·8	27·3	16·0	9·3	9·15	31·0	11·0	9·8	12·1	13·9	15·4	12·7	13·9	12·4
Eu	1·30	0·45	0·97	0·84	0·90	1·22	0·65	0·47	0·48	0·82	0·32	0·26	1·31	1·42	1·55	4·77	4·91	4·73
Gd	22·0	14·4	25·3	29·5	28·7	26·9	22·8	8·35	7·89	24·7	9·57	8·34	11·3	12·7	13·9	12·0	12·9	12·1
Tb	3·85	3·01	3·78	4·56	4·52	4·32	4·63	1·27	1·27	3·57	1·49	1·28	1·78	2·01	2·19	1·74	1·88	1·65
Dy	23·3	20·0	22·7	25·6	25·6	24·6	29·5	7·24	7·13	18·9	8·56	7·35	10·18	11·4	12·3	9·22	10·23	8·79
Ho	4·85	4·27	4·70	5·16	5·06	4·85	6·07	1·45	1·44	3·69	1·74	1·52	2·02	2·31	2·46	1·72	2·03	1·72
Er	13·5	12·3	13·9	14·4	14·2	13·2	16·7	4·36	4·23	10·09	5·04	4·67	5·76	6·45	6·94	4·13	4·61	3·82
Yb	11·6	11·5	13·3	13·2	13·3	11·8	13·6	5·06	5·06	9·52	5·25	5·43	5·44	6·19	6·39	3·22	3·96	3·19
Lu	1·66	1·65	1·92	1·87	1·89	1·62	1·97	0·80	0·79	1·43	0·83	0·83	0·83	0·94	1·01	0·44	0·57	0·48

Sample:	64R1 127–135	64R1 136–146	64R2 78–87	64R3 96–105	64R4 103–115	64R4 128–137	65R1 69–76	65R3 15–19	65R3 129–134	66R1 11–18	66R3 2–10	66R3 70–84	66R5 79–86	67R4 35–41	67R4 113–125	67R5 48–55	68R4 17–24	69R1 92–97
Unit:	7	7	7	7	8	8	9	10	10	11	12	12	13	14	14	14	15	16
Rock type:	BTA	BTA	BTA	TB	TB	TB	TB	BTA	TB	BTA	TB	TB	Te	TB	PT	BTA	Te	BTA
Depth (mbsf):			606	608	610	614	615	620	625	622	625	630	632	635	636	638	647	653
SiO_2			53·4	47·6	48·3	49·1	48·8	51·2	50·8	50·8	49·4	49·0	47·1	46·8	51·2	52·1	47·1	51·6
TiO_2			2·92	3·41	3·95	4·12	4·19	4·97	4·85	4·14	4·19	4·36	4·49	2·27	2·65	2·79	3·67	2·90
Al_2O_3			17·5	14·9	14·4	15·1	15·7	17·4	17·4	16·5	15·4	15·9	16·8	14·0	16·9	17·2	16·5	14·9
Fe_2O_3			9·65	17·4	14·0	13·2	15·6	10·3	12·6	11·5	12·1	12·1	11·6	23·4	12·8	9·98	13·6	12·3
MnO			0·37	0·49	0·26	0·30	0·27	0·18	0·47	0·24	0·17	0·24	0·28	0·62	0·33	0·23	0·33	0·20
MgO			1·00	2·49	4·27	3·30	1·74	1·89	2·05	1·57	3·22	1·39	1·30	2·34	1·17	0·91	1·27	2·53
CaO			5·58	6·33	7·63	7·20	5·72	6·08	4·45	6·48	7·12	8·27	9·93	3·48	4·92	6·37	8·10	7·21
Na_2O			4·59	3·04	3·57	3·77	3·71	3·67	2·81	3·68	3·94	3·88	3·84	2·56	4·51	4·64	4·11	3·38
K_2O			3·65	2·52	2·24	2·38	2·57	2·59	2·55	2·86	2·63	2·71	3·05	3·29	4·07	3·99	3·26	2·93
P_2O_5			1·08	1·43	0·98	1·03	1·22	1·12	1·11	1·67	1·58	1·65	1·23	0·96	1·11	1·16	1·38	1·15
Total			99·7	99·6	99·6	99·5	99·5	99·3	99·0	99·4	99·8	99·5	99·6	99·7	99·6	99·4	99·3	99·2
LOI			5·98	14·1	3·48	4·42	8·99	10·4	10·7	5·95	5·53	9·23	8·91	15·7	8·23	6·00	8·65	4·36
Rb	50·3	50·5	63·1	29·6	38·1	44·6	41·2	50·3	51·2	49·5	42·5	45·1	49·1	43·6	59·7	61·9	52·1	42·2
Cs	0·21	0·21	0·74	0·69	0·25	0·23	0·25	0·60	0·76	0·19	0·13	0·27	0·27	0·76	0·33	0·41	0·20	0·17
Sr	443	444	480	255	422	473	447	452	389	521	509	538	569	160	465	533	477	428
Ba	1513	1513	1417	1096	739	840	836	882	822	1018	959	1040	1170	1120	2202	2115	938	898
Hf	8·47	8·57	8·81	7·15	6·99	7·55	7·55	8·45	8·43	8·79	7·63	7·94	8·03	7·52	8·05	8·02	9·03	8·54
Zr	373	374	421	345	315	345	341	377	377	369	341	346	369	340	396	400	398	376
Ta	2·69	2·70	2·84	2·30	2·23	2·47	2·60	2·87	2·80	2·96	2·47	2·72	2·66	2·50	2·24	2·19	2·84	2·56
Nb	44·6	45·0	52·0	40·3	37·3	42·4	43·5	49·0	47·5	47·5	40·7	45·3	44·6	42·5	38·8	38·2	47·3	40·5
U	0·82	0·84	0·91	0·49	0·84	0·81	0·54	0·52	0·61	0·43	0·49	0·59	0·79	0·52	0·91	0·99	0·52	0·92
Th	4·21	4·26	3·81	2·93	3·10	3·20	3·23	3·64	3·55	3·68	3·17	3·33	3·35	3·80	3·99	3·88	4·57	3·76
Pb	5·90	5·80	6·95	5·99	5·10	4·95	5·89	5·56	6·15	5·16	4·77	5·31	6·25	7·10	7·21	7·42	6·46	6·38
Y	47·6	47·3	51·4	53·3	42·3	45·5	45·6	48·8	46·7	53·6	52·3	52·6	50·3	59·0	49·2	52·7	57·3	49·2
Ni				3·49	9·33	6·28		10·05	11·2		3·18	1·10	3·29	2·37	1·09	1·06	1·10	1·05
Cr				4·66	25·9	8·37		16·8	17·9		75·2	50·7	2·20	3·56	5·45	—	6·57	2·09
V				171	290	308		334	381		240	258	285	159	90	95	207	134
La	50·2	49·5	57·3	51·7	40·9	46·7	47·5	49·8	49·0	55·5	51·4	55·1	51·3	50·4	56·0	58·2	55·8	49·7
Ce	105	104	118	111·2	85·9	98·4	100·0	104·3	102·7	119	110	116	107·5	104	117	121	119	103·3
Pr	13·1	13·2	14·7	14·3	11·0	12·3	12·9	13·2	12·8	15·3	14·1	15·1	13·7	13·2	14·6	15·2	15·2	13·0
Nd	53·2	52·7	60·3	60·9	46·4	51·5	54·4	55·3	53·9	66·2	61·2	65·1	57·4	53·9	60·4	62·9	62·9	55·4
Sm	11·0	11·1	12·4	13·1	9·8	10·9	11·5	11·8	11·3	14·0	13·0	13·9	12·2	11·5	12·4	12·8	13·4	11·7
Eu	4·75	4·76	4·80	5·11	3·32	3·72	3·87	4·10	3·98	5·12	4·82	5·10	4·61	4·87	5·74	5·79	4·01	3·67
Gd	11·0	11·0	12·2	13·2	10·01	10·9	11·3	11·6	11·00	13·9	13·2	14·0	12·2	11·6	12·0	12·8	13·0	11·5
Tb	1·56	1·56	1·69	1·83	1·44	1·54	1·61	1·67	1·58	1·99	1·86	1·93	1·74	1·74	1·71	1·80	1·87	1·63
Dy	8·66	8·59	9·26	9·95	8·02	8·23	9·19	9·15	8·71	10·9	9·92	10·17	9·38	9·79	9·41	9·98	10·41	9·35
Ho	1·68	1·67	1·81	1·88	1·52	1·60	1·75	1·72	1·64	2·05	1·91	1·90	1·77	1·97	1·79	1·88	2·02	1·80
Er	4·62	4·52	4·27	4·57	3·61	3·79	4·23	4·15	4·00	4·88	4·43	4·52	4·32	5·47	4·36	4·59	5·29	4·35
Yb	3·73	3·66	3·80	4·11	3·22	3·36	3·76	3·55	3·43	4·12	3·83	3·76	3·87	4·85	3·91	3·98	4·20	3·84
Lu	0·55	0·54	0·58	0·63	0·48	0·50	0·54	0·49	0·50	0·60	0·55	0·54	0·54	0·74	0·60	0·60	0·62	0·57

Table 1: continued

Sample:	69R2 105–109	70R4 108–118	71R2 14–21	71R4 40–50	71R4 40–50	71R6 96–104	72R2 25–35	73R3 100–111	BHVO-1 Average of 27 analyses	BHVO-1 Eggins *et al.* (1997)	BR Average of 8 analyses	BR Eggins *et al.* (1997)	RGM-1 Average of 8 analyses	RGM-1 Eggins *et al.* (1997)	BHVO-1 Calibration values
Unit:	17	18	18	18	18	19	19	19							
Rock type:	BTA	Tr	Tr	Tr	Dup.	Tr	Tr	Tr							
Depth (mbsf):	660	672	674	676		678	682	693							
SiO_2	52·1	62·0	64·1	63·9		70·3	70·5	69·3							
TiO_2	3·15	0·81	0·81	0·56		0·45	0·43	0·46							
Al_2O_3	16·3	15·1	14·9	16·9		13·5	13·2	13·4							
Fe_2O_3	10·9	11·5	8·83	9·09		6·17	5·75	6·67							
MnO	0·18	0·31	0·44	0·02		0·12	0·17	0·21							
MgO	1·91	0·61	0·37	0·56		0·24	0·15	0·16							
CaO	6·18	0·67	1·06	0·21		0·62	0·42	0·14							
Na_2O	4·01	3·41	3·78	4·08		3·38	3·72	3·78							
K_2O	3·26	5·41	5·65	4·48		4·90	5·24	5·17							
P_2O_5	1·24	0·15	0·16	0·06		0·03	0·01	0·02							
Total	99·2	100·0	100·1	99·8		99·7	99·6	99·3							
LOI	4·24	6·81	5·32	3·86		2·98	2·90	3·33							
Rb	54·3	58·5	63·3	60·4	61·0	117·4	115	115	9·13	9·50	51·4	47	145	149	9·20
Cs	0·22	0·2	0·12	0·70	0·76	0·4	0·26	0·36	0·10	0·10	0·81	1	9·9	9·60	0·10
Sr	468	15·3	15·8	41·2	42·1	14·4	9·65	11·8	395	390	1294	1320	102	108	399
Ba	980	165·3	207	103·0	105	88·7	65·0	50·5	132	133	1006	1050	824	807	132·9
Hf	9·10	10·1	10·6	35·8	36	27·5	28·7	26·2	4·47	4·30	5·85	5·62	6·11	6·20	4·49
Zr	415	449	464	1604	1613	1260	1253	1216	182	180	290	250	240	219	184
Ta	2·81	3·2	3·25	9·13	9·46	7·3	7·37	6·75	1·20	1·20	5·37	5·79	0·95	0·95	1·21
Nb	45·7	54·0	55·9	163	163	122·7	121	120	19·4	19·5	112	98	9·41	8·90	19·7
U	0·99	0·7	1·13	1·54	1·63	1·1	2·62	2·05	0·41	0·42	2·23	2·46	5·38	5·80	0·41
Th	4·18	5·6	5·69	18·6	19·8	15·3	15·0	13·2	1·25	1·26	9·95	10·87	14·9	15·1	1·25
Pb	6·51	7·0	5·63	28·3	21·1	14·5	15·4	13·2	2·06	2·10	4·65	4·77	28·4	24·0	2·06
Y	53·0	51·8	54·8	113	112	58·1	164	232	27·8	28·0	31·3	30	24·3	25·0	28·0
Ni	1·04	—	—	—		—		1·03							
Cr	—	93·3	—	3·12		7·22		—							
V	143	—	—	—		—		—							
La	54·9	55·2	55·5	107	109	75·8	170	288	15·5	15·5	77·3	82	22·8	27·0	15·5
Ce	113	118·4	112	277	328	239·3	165	338	37·7	38·0	145	151	45·1	47·0	38·0
Pr	14·3	14·9	14·7	28·1	28·9	17·4	46·8	66·6	5·42	5·45	16·7	17·36	5·27	5·30	5·45
Nd	60·4	59·5	59·2	108	110	65·6	177	244	24·6	24·7	63·6	65	19·0	19·0	24·7
Sm	12·6	12·8	12·7	23·0	23·8	13·8	35·2	44·4	6·17	6·17	11·8	12	3·96	4·30	6·17
Eu	4·03	2·9	2·79	1·98	2·03	1·3	2·60	3·38	2·05	2·06	3·5	3·7	0·55	0·66	2·06
Gd	12·6	11·7	11·8	21·0	21·2	13·1	30·8	42·6	6·17	6·22	10·0	9·5	3·76	3·70	6·22
Tb	1·77	1·8	1·87	3·42	3·50	2·1	4·99	5·96	0·95	0·95	1·28	1·25	0·60	0·66	0·95
Dy	10·01	9·9	10·31	20·0	20·2	11·2	29·3	33·7	5·27	5·25	6·22	6·20	3·61	4·08	5·25
Ho	1·93	1·9	2·03	4·01	4·08	2·2	5·91	7·08	1·00	1·00	1·08	1·087	0·77	0·95	1·00
Er	4·64	5·2	5·55	11·1	11·1	6·1	16·1	19·1	2·57	2·56	2·60	2·4	2·32	2·60	2·56
Yb	4·08	4·8	5·26	9·57	9·88	6·8	12·5	12·7	1·99	1·98	1·8	1·9	2·47	2·60	1·98
Lu	0·60	0·8	0·85	1·34	1·37	1·1	1·73	1·84	0·28	0·28	0·3	0·25	0·38	0·41	0·28

Major (in wt %) and trace element (in ppm) data. Averages of standard values are reported together with Eggins *et al.* (1997) preferred values. BHVO-1 calibration values used during this study are a compilation of data from Eggins *et al.* (1997) and T. Plank (personal communication, 2000). —, values below limit detection; blanks indicate that the element was not measured. TB, trachybasalt; BTA, basaltic trachyandesite; Te, tephrite; D, dacite; Tr, trachyte; R, rhyolite; PT, phonotephrite; Dup., duplicate; mbsf, metres below sea floor. All the data, major and trace elements, are normalized to the measured oxide total on a volatile-free basis. Normalization was not possible for two samples (64R1 127–135 and 64R1 136–146) that lack major element data.

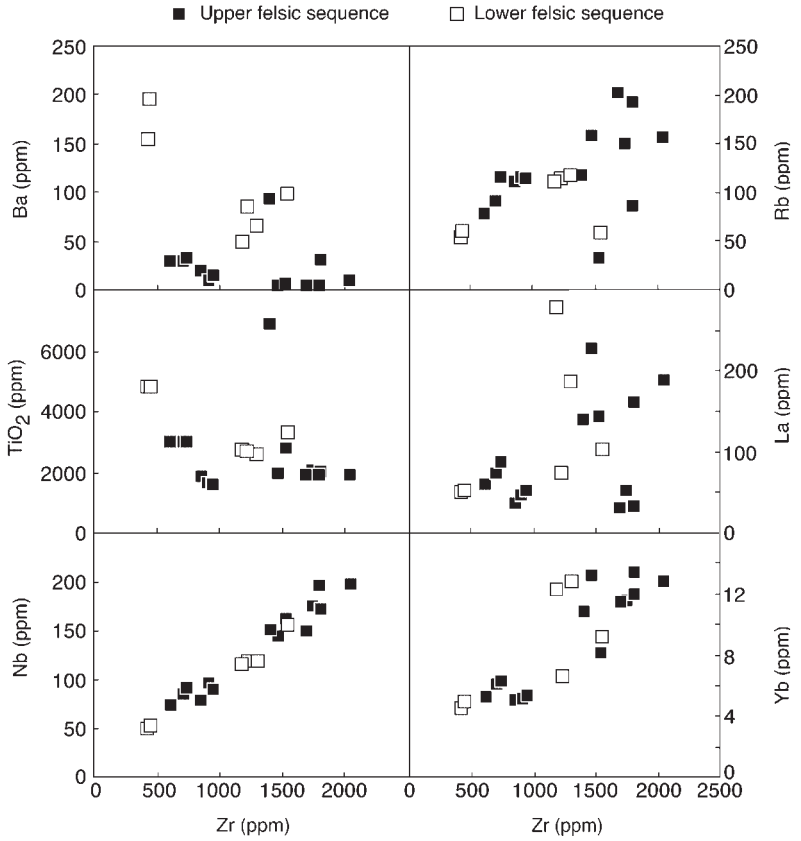

Fig. 3. Variation diagrams illustrating a good correlation in the felsic rocks between two immobile elements (Zr and Nb) and poor correlation between other pairs of elements. In some cases the poor correlation results from mobility during alteration (e.g. Rb vs Zr), in some cases it is the result of variable extents of fractional crystallization (TiO_2 vs Zr), and in the other cases both processes are implicated.

and alkalic rocks (Kuno, 1966). A notable exception is the altered vitric tuff (Unit 3), which plots in the tholeiitic domain, in the field of dacite.

Stratigraphic variations in major and trace element compositions, from base to top of the drilled section, are illustrated in Fig. 5a and b. The mafic–felsic bimodality of the volcanic suites is immediately apparent. The mafic lavas have a restricted range of relatively low SiO_2 contents, from 46 to 54 wt %, and the felsic rocks show a wider range, from 61 to >80 wt %. There is little systematic up-section evolution in major and trace element compositions, and few differences between compositions in the upper and lower felsic suites. An exception is Al_2O_3, which is lower in rhyolites in the upper part of the section than in trachyte flows from both the lower part of the upper felsic series (Unit 5) and from the lower series (Units 18 and 19).

The highly altered green vitric tuff (sample 56R3 101–107; Unit 3) again plots separately from the other samples. It has unusually high MgO, Al_2O_3, P_2O_5, LOI, Cs, Sr, REE and Y, and low K_2O, Na_2O and Rb (Fig. 5a and b).

In the variation diagrams (Fig. 6a and b), the samples also fall into two distinct groups. Concentrations of most major elements in the high-SiO_2 felsic rocks are distinctly lower than in the trachybasalts. Elements that are incompatible with ferromagnesian minerals, such as Th, Zr and most of the REE, are present in high concentrations in the felsic rocks, whereas elements compatible with feldspar (Sr, Eu and Ba) or minor mineral phases (Ti, P) are relatively depleted.

In the REE and mantle-normalized trace element diagrams plotted as Fig. 7, the felsic volcanic rocks plot as relatively smooth spectra punctuated by large troughs (negative anomalies) at Ba, Sr, Eu, Ti and P. A notable feature is the relatively flat slope of the more compatible elements and the relatively wide range in the concentrations for these elements. Ytterbium contents, for example, vary by a factor of about three, from 5 to 13·5 ppm. This behaviour is shown more specifically in Fig. 8, in which a heavy REE (HREE) ratio $(Gd/Yb)_N$ is plotted against the concentrations of light REE (LREE) and HREE. Three samples of rhyolite from Unit 1 in the upper sequence (51R1 13–19, 52R1 2–7 and 54R1

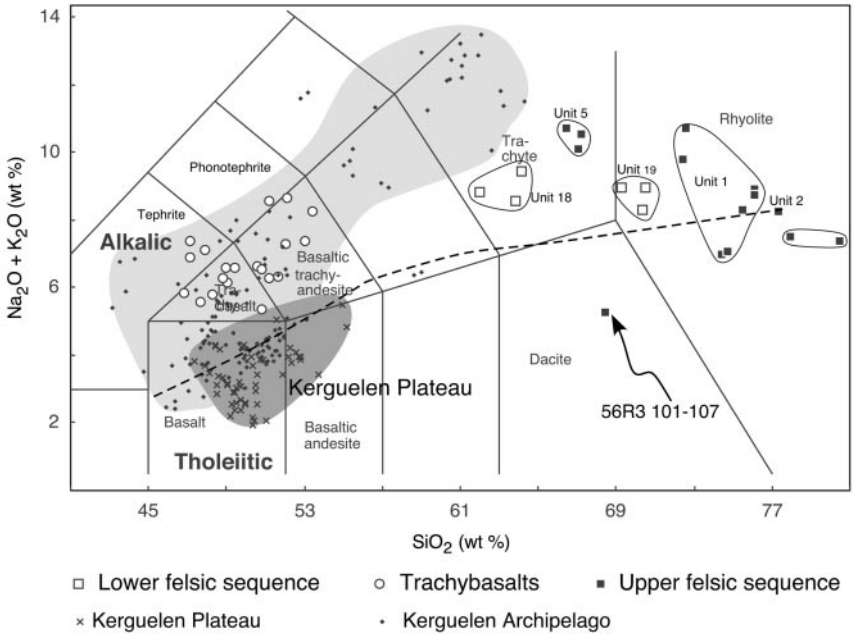

Fig. 4. Total alkalis ($Na_2O + K_2O$) vs SiO_2 diagram after Le Bas *et al.* (1986). Fields representing rocks from the Kerguelen Archipelago are from Weis *et al.* (1993, 1998), Yang *et al.* (1998) and Frey *et al.* (2000*b*). Those for the Kerguelen Plateau are from Salters *et al.* (1992), Storey *et al.* (1992), Shipboard Scientific Party (2000) and Frey *et al.* (2002). The tholeiitic–alkalic dividing line is from Kuno (1966). Numbers on samples or open fields identify the volcanic units from Site 1139 (see Fig. 2).

1–9) have trace element patterns very different from those of the other felsic rocks. They all have relatively low abundances of LREE, but their HREE are as high as, or higher than those in the other samples. This behaviour is also illustrated in Fig. 8, in which $(La/Sm)_N$ is plotted against $(Gd/Yb)_N$. It is notable that the samples with relatively low LREE have the lowest Ba, Sr, Eu and P contents. These samples are relatively rich in spherulitic textured glass, and they may have been more susceptible to alteration than the other samples.

Another group of elements, including Cs, U, Rb and Ce, shows wide variation that appears decoupled from normally immobile elements such as Th and Zr (Fig. 8a and b). As mentioned in the introduction to this section, this scatter is probably due to mobility of these elements during alteration of the rocks.

In contrast to the diversity of trace element patterns of the felsic rocks, all the trachybasalts have very similar patterns (Figs 6 and 7). They are depleted in HREE compared with middle REE (MREE) to LREE [$(Gd/Yb)_N$ = 2–3·1] and have strongly sloping trace element patterns. Levels of LREE are similar to those in the least-enriched felsic lavas. All samples have low Cs contents, large negative Th and U anomalies, and small but variable Nb, Pb, Sr and Ti anomalies (Fig. 7). Small positive Ba and Eu anomalies are present in some samples. As discussed in a later section, these variations are due in part to alteration, in part to fractional crystallization, and perhaps in part to source characteristics.

In the trace element correlation diagrams (Fig. 8a and b), the mafic and felsic rocks again show contrasting patterns. Only for a few elements is there a close correlation (e.g. Zr, Th and Nb). In the Ti vs Zr diagram, two very different trends are seen: in the mafic lavas Ti varies widely whereas Zr remains constant; in the felsic lavas, Ti is more constant whereas Zr varies. A similar pattern is seen when Ba, Eu, Sr, P and Pb are plotted against Zr or La.

Isotopic compositions

Isotopic data are listed in Table 2 and plotted in Figs 9 and 10. Measured values in the mafic lavas are relatively uniform; except for three samples with slightly higher Nd isotope ratios, $^{143}Nd/^{144}Nd$ ranges only from 0·51251 to 0·51259 and $^{87}Sr/^{86}Sr$ from 0·7057 to 0·7071. Initial isotope ratios were calculated for an age of 68 Ma, using element ratios measured by ICP-MS on unleached powders. Initial neodymium isotope ratios ($^{143}Nd/^{144}Nd)_{68\,Ma}$ range from 0·51246 to 0·51271 ($\varepsilon Nd_{68\,Ma}$ = 3·0 to −1·8) and initial strontium ratios ($^{87}Sr/^{86}Sr)_{68\,Ma}$ from 0·7054 to 0·7059.

The felsic samples have a restricted range of Nd isotope compositions (0·51250–0·51262) that coincides with values in the mafic lavas. Initial ($^{143}Nd/^{144}Nd)_{68\,Ma}$ calculated

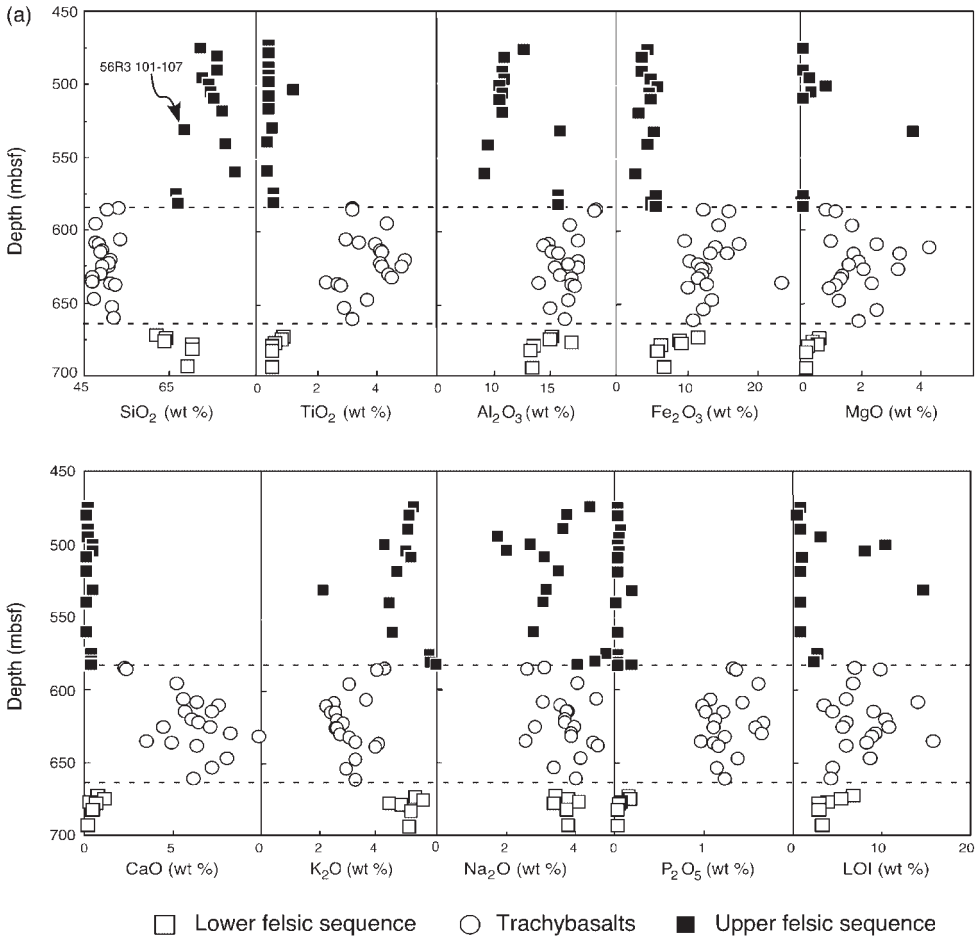

Fig. 5.

using Sm/Nd ratios measured by ICP-MS in the whole-rock powders range from 0·51245 to 0·51257. Strontium isotope ratios measured on leached powders show an enormous range, from 0·7105 to 1·58; measurements of two unleached samples, in contrast, gave values that are still very high, but in a more restricted range (0·7810–0·7912). The leachates gave values between 0·7108 and 0·7269.

Measured lead isotope compositions are plotted in Fig. 10. The felsic volcanic rocks have slightly higher $^{206}Pb/^{204}Pb$ than the mafic lavas (17·6–17·9 compared with 17·5–17·6). The same relationship is seen for $^{208}Pb/^{204}Pb$, but not for $^{207}Pb/^{204}Pb$. When initial Pb isotope compositions are calculated using U/Pb from the ICP-MS analyses and an age of 68 Ma, two samples of felsic rock plot within the field of the mafic lavas, but the remainder plot as a separate group, still with slightly higher $^{206}Pb/^{204}Pb$ and $^{208}Pb/^{204}Pb$.

COMPARISON WITH OTHER PARTS OF THE KERGUELEN PLATEAU

The alkalic character and the high concentrations of incompatible trace elements of samples from Site 1139 distinguish them from the majority of volcanic rocks of the Kerguelen Plateau, which are flood basalts with tholeiitic compositions (Salters *et al.*, 1992; Storey *et al.*, 1992; Weis & Frey, 2002). The Site 1139 samples more closely resemble some of the younger (<10 Ma) rocks on the Kerguelen Archipelago (Fig. 11). As described by Weis *et al.* (1993), Yang *et al.* (1998), Frey *et al.* (2000*b*) and Doucet *et al.* (2002), the Archipelago consists mainly of two series of flood basalts, an older 30–28 Ma series with a tholeiitic to transitional character, and a younger ~25–24 Ma alkalic series. These rocks are overlain by much younger (<10 Ma) alkalic lavas and volcaniclastic rocks, particularly in the South East Province (Gautier

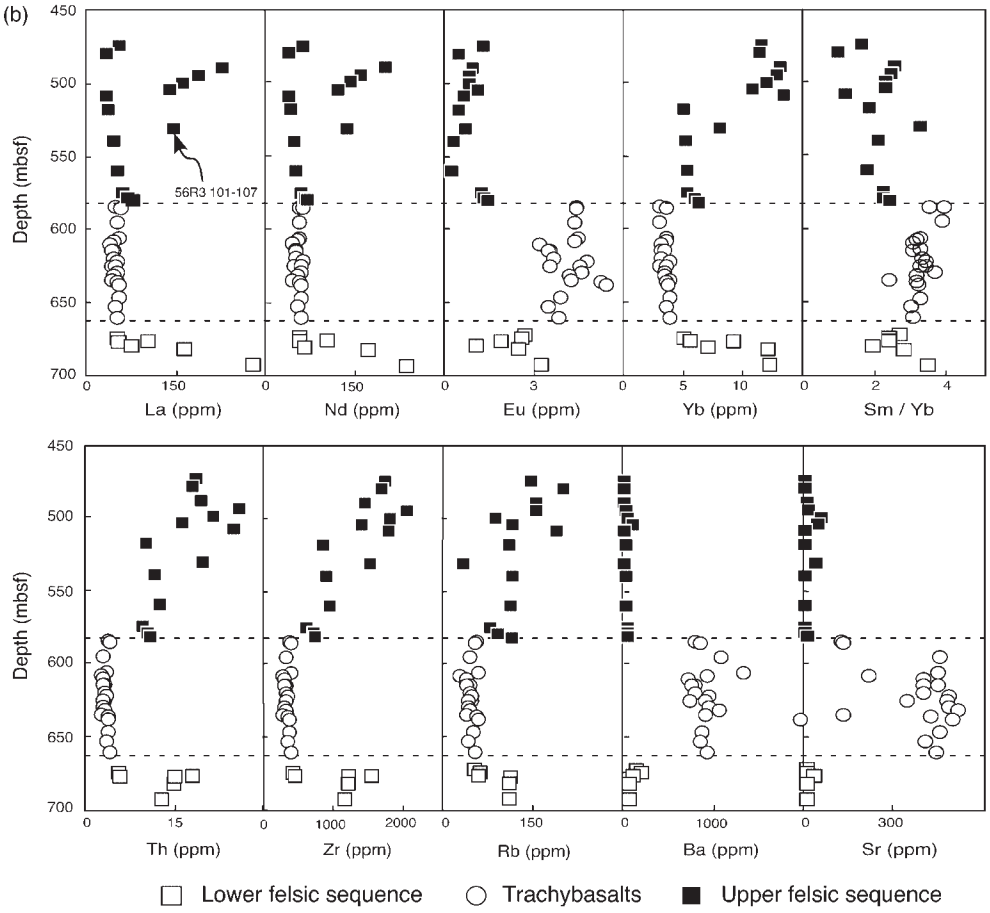

Fig. 5. Downcore variations in major (a) and trace element (b) concentrations.

et al., 1990; Weis *et al.*, 1993) and Mt Ross (Weis *et al.*, 1998). Differentiated suites of mafic to felsic alkalic rocks erupted as part of the still-active volcanism on Heard Island (Barling *et al.*, 1994).

Large differences exist between the compositions of the trachybasaltic lavas from Site 1139 and those of mafic lavas from other locations on the Kerguelen Plateau and Archipelago. In Fig. 11, the trachybasalts are seen to have low contents of MgO (4·3–0·7%) and CaO (2·2–9·9%), which causes them to plot separately from rocks from throughout the Kerguelen Plateau and Archipelago. In addition, some Site 1139 samples have unusually high Fe_2O_3 and P_2O_5 contents.

In Fig. 9, the Nd and Sr isotope ratios of mafic lavas from Site 1139 plot close to the trend of Heard Island lavas and near those of basalts of Sites 747, 748 and 1137, which are all located in the central part of the Kerguelen Plateau (Salters *et al.*, 1992; Barling *et al.*, 1994; Weis *et al.*, 2001; Frey *et al.*, 2002; Ingle *et al.*, 2002). The isotopic compositions also are similar to those of younger alkaline lavas from the Kerguelen Archipelago (Weis *et al.*, 1993, 1998; Frey *et al.*, 2000*b*). Strongly negative initial εNd values, like those of crust-contaminated lavas from Site 738 (Mahoney *et al.*, 1995), are absent.

In Pb/Pb diagrams (Fig. 10), the measured isotopic compositions of the mafic lavas from Site 1139 plot at the high $^{207}Pb/^{204}Pb$ end of the fields defined by Sites 747 and 750 (Salters *et al.*, 1992; Frey *et al.*, 2002). Both the mafic and the felsic rocks have compositions near the unradiogenic end of Heard Island trend, close to the compositions of Site 749 but with higher $^{208}Pb/^{204}Pb$ vs $^{206}Pb/^{204}Pb$. In Site 1139 lavas, $^{206}Pb/^{204}Pb$ and $^{208}Pb/^{204}Pb$, but not $^{207}Pb/^{204}Pb$, are distinctly lower than in rocks from the Kerguelen Archipelago (Weis *et al.*, 1993, 1998; Yang *et al.*, 1998; Frey *et al.*, 2000*b*).

DISCUSSION

Effects of alteration on the compositions of the mafic lavas

Many chemical characteristics of the volcanic rocks from Site 1139 can be attributed to fractional crystallization

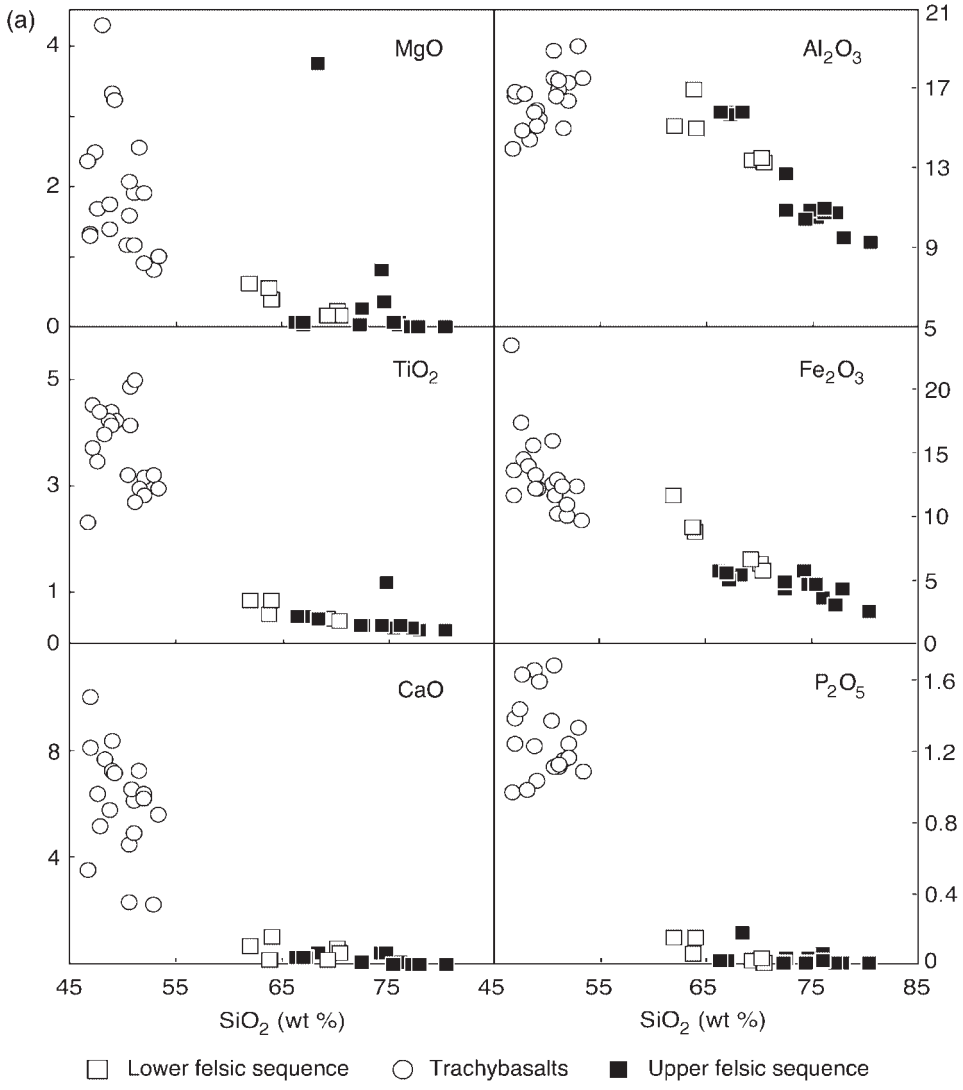

Fig. 6.

of the phenocryst phases in the lavas. The relatively evolved, trachybasaltic (rather than basaltic) chemical compositions of the mafic lavas are broadly consistent with their mineral assemblages, which have high feldspar contents and low abundances of ferromagnesian minerals. For example, the mineral modes of the trachybasalts contain 70–80% feldspar, 0–3% mafic minerals, 5–10% Fe–Ti oxides and 10–20% clay minerals. As explained above, the oxides are interpreted to represent the altered relicts of mafic minerals such as clinopyroxene or amphibole. Because of this alteration, it is difficult to obtain reliable information about the original magmatic mineralogy.

It is probable that these rocks acquired their evolved character, at least in part, by fractional crystallization of more mafic, basaltic, parental magmas. None the less, their peculiar position in the variation diagrams (Fig. 11), where they plot apart from the mafic to felsic volcanic series of the Kerguelen Archipelago (Weis *et al.*, 1993, 1998; Yang *et al.*, 1998; Frey *et al.*, 2000*b*) probably has another cause. Comparison of petrographic features of lavas of the younger suites from the Kerguelen Archipelago and Site 1139 reveals few differences in the inferred primary mineral assemblages (Weis *et al.*, 1998; Frey *et al.*, 2000*b*). What distinguishes the two is the degree of alteration, particularly the almost complete replacement of primary ferromagnesian minerals in Site 1139 lavas by an assemblage of clay minerals and Fe oxides.

To estimate the pre-alteration composition of the mafic lavas we made four assumptions: (1) the lavas originally had major element compositions that plotted

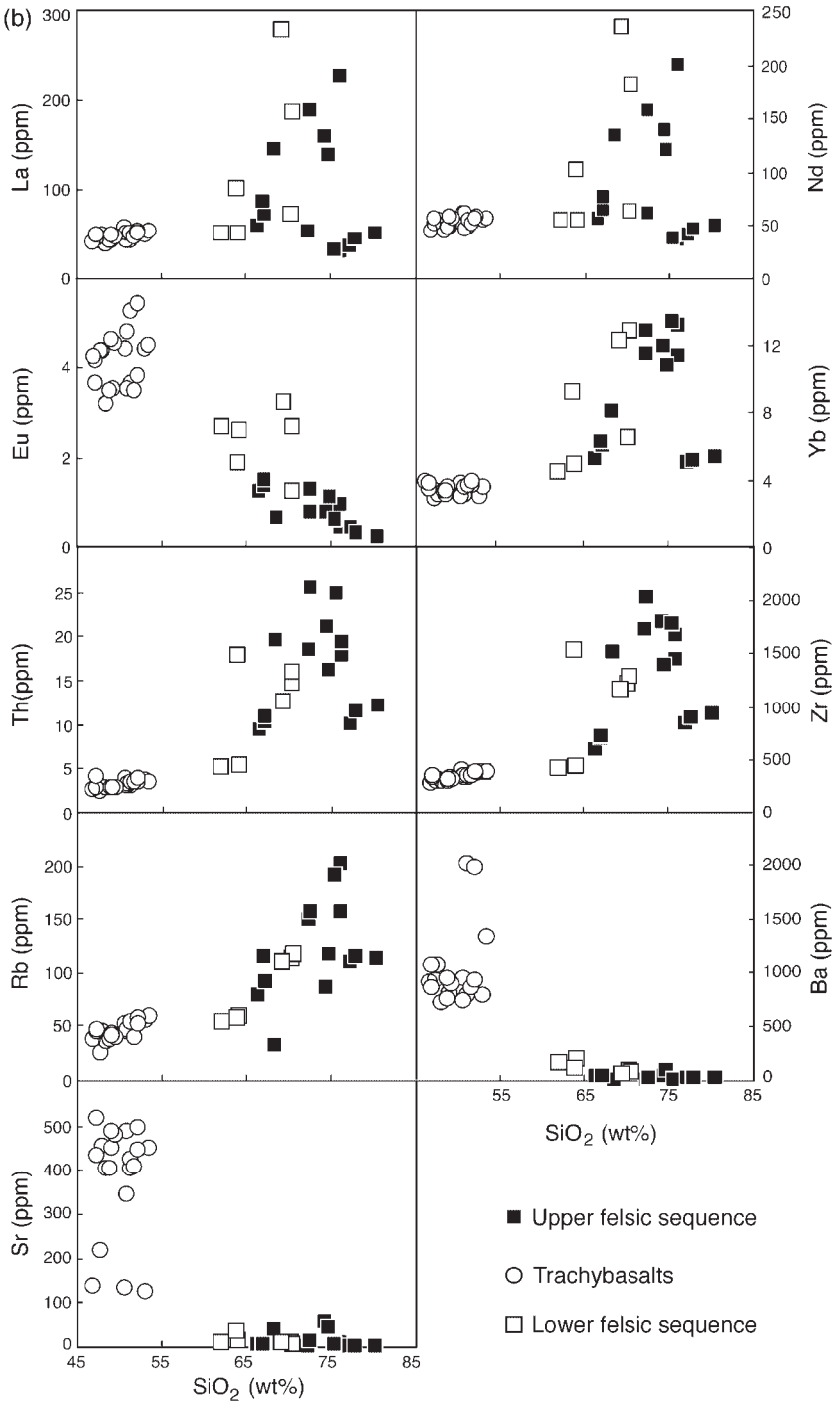

Fig. 6. Variation diagrams of major elements (a) and trace elements (b) vs silica.

on the broad trend defined by lavas from the Kerguelen Archipelago; (2) Zr was immobile during alteration; (3) the pre-alteration Zr contents of the Site 1139 rocks were similar to those of Kerguelen Archipelago lavas; (4) orthopyroxene was absent from the norm of these alkalic rocks. As shown in Fig. 12 for MgO, we added MgO and CaO, and subtracted FeO from the compositions of Site 1139 lavas until their compositions plotted within the trend of the Archipelago samples, and refined the adjustment until orthopyroxene was

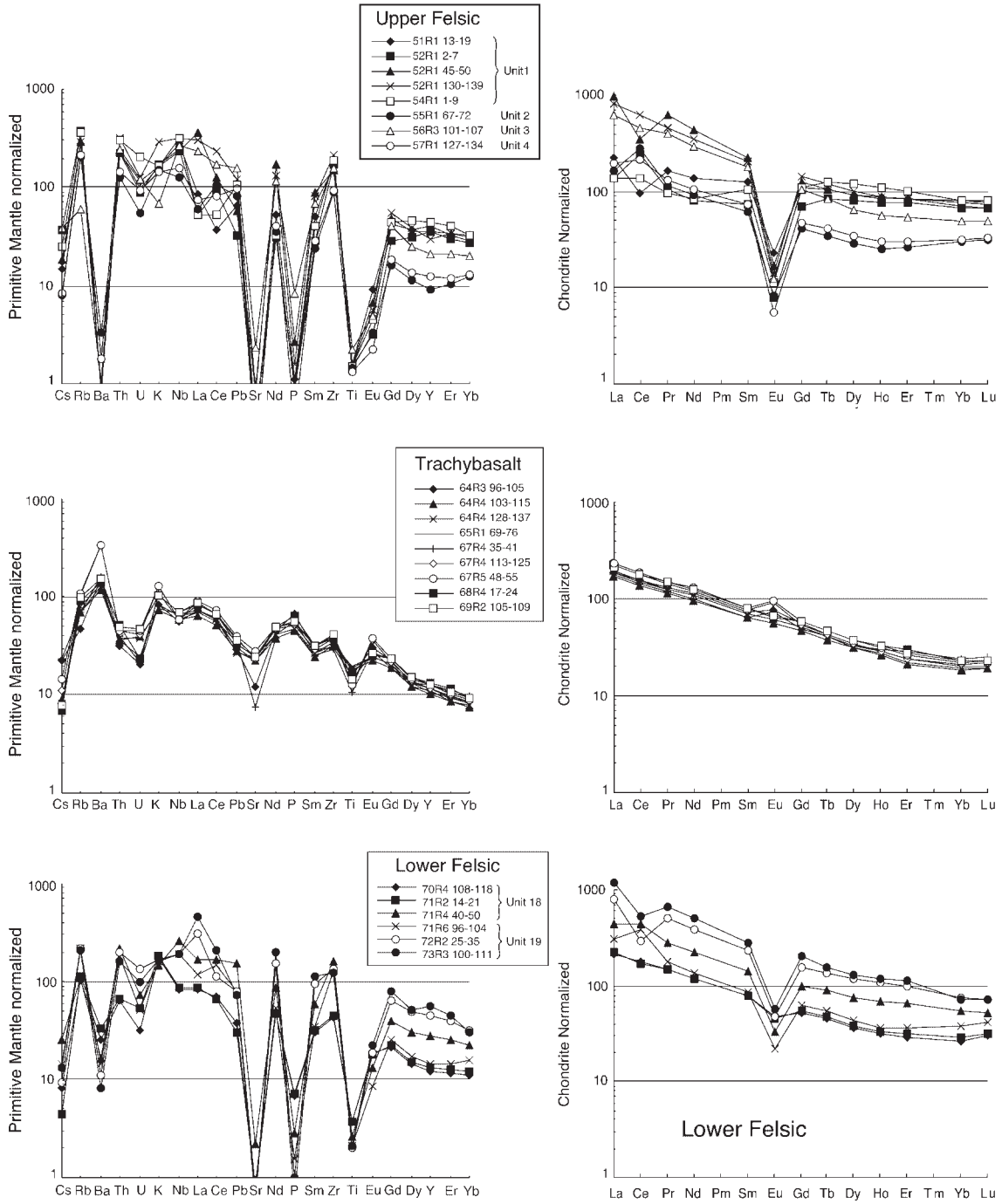

Fig. 7. Rare earth elements and mantle-normalized trace elements. The REE were normalized to chondrites using values from Sun & McDonough, (1989); trace elements to primitive mantle using values of Hofmann (1988). For the upper felsic series and trachybasalts, only representative samples are shown.

eliminated from the norm. No adjustments were made to the other elements, except to renormalize the compositions to 100%. After correction, the rocks retain their principal chemical characteristics; in the total alkalis vs SiO_2 diagram, for example, they still plot within or near the trachybasalt field and still lie in the alkalic domain. The normative mineralogical assemblage corresponding to the adjusted composition contains, on average, 11% olivine, 12% clinopyroxene, 44% plagioclase and 18% orthoclase.

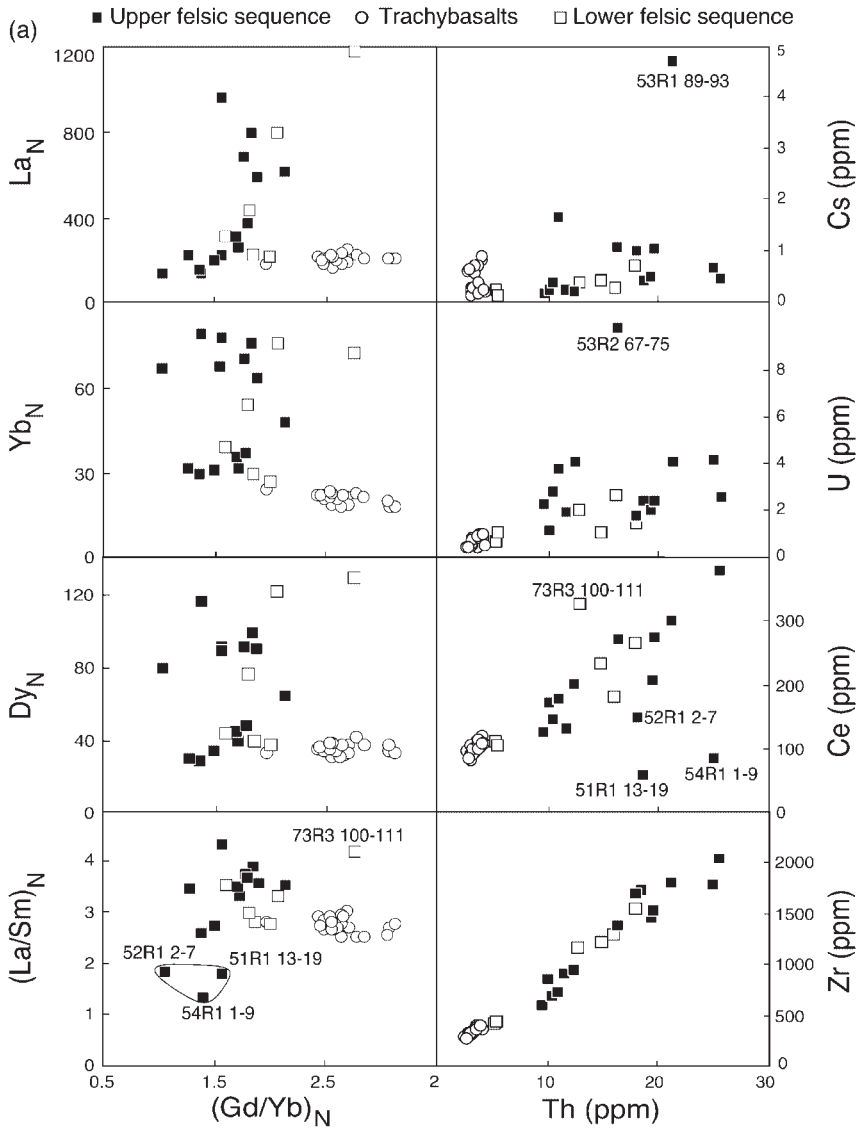

Fig. 8.

The relatively uniform abundances and ratios, in the entire trachybasalt suite, of REE, HFSE (except for Ti) and Th suggest that these elements were little affected by alteration. All these rocks have very similar REE patterns (Fig. 7) and plot in a very tight group in Fig. 8a. The greater scatter of Cs and U in Fig. 8a indicates, in contrast, that these elements were mobile. In Figs 7 and 8b, Sr and Eu also scatter widely, probably because of a combination of alteration and feldspar fractionation. The large variation of Ti and P contents, which is partially responsible for the contrasting trends for mafic and felsic lavas in Fig. 8b, can be attributed to fractionation of Fe oxides and apatite.

Origin of the mafic lavas

The steeply sloping trace element patterns and the high concentrations of the more incompatible elements can be interpreted as the result of either (1) low-degree mantle melting under conditions that left garnet as a residual phase or (2) partial melting of a source that itself was enriched and had sloping REE patterns. The initial Nd isotopic compositions range from 0·51246 to 0·51271 ($\varepsilon Nd_{68\,Ma} = +3$ to $-1{\cdot}8$), but the majority have relatively constant low values around 0·51247. The relative constancy of Sr and Pb isotopic compositions, as illustrated in Figs 9 and 10, suggests that these compositions may not been greatly affected by alteration. These values

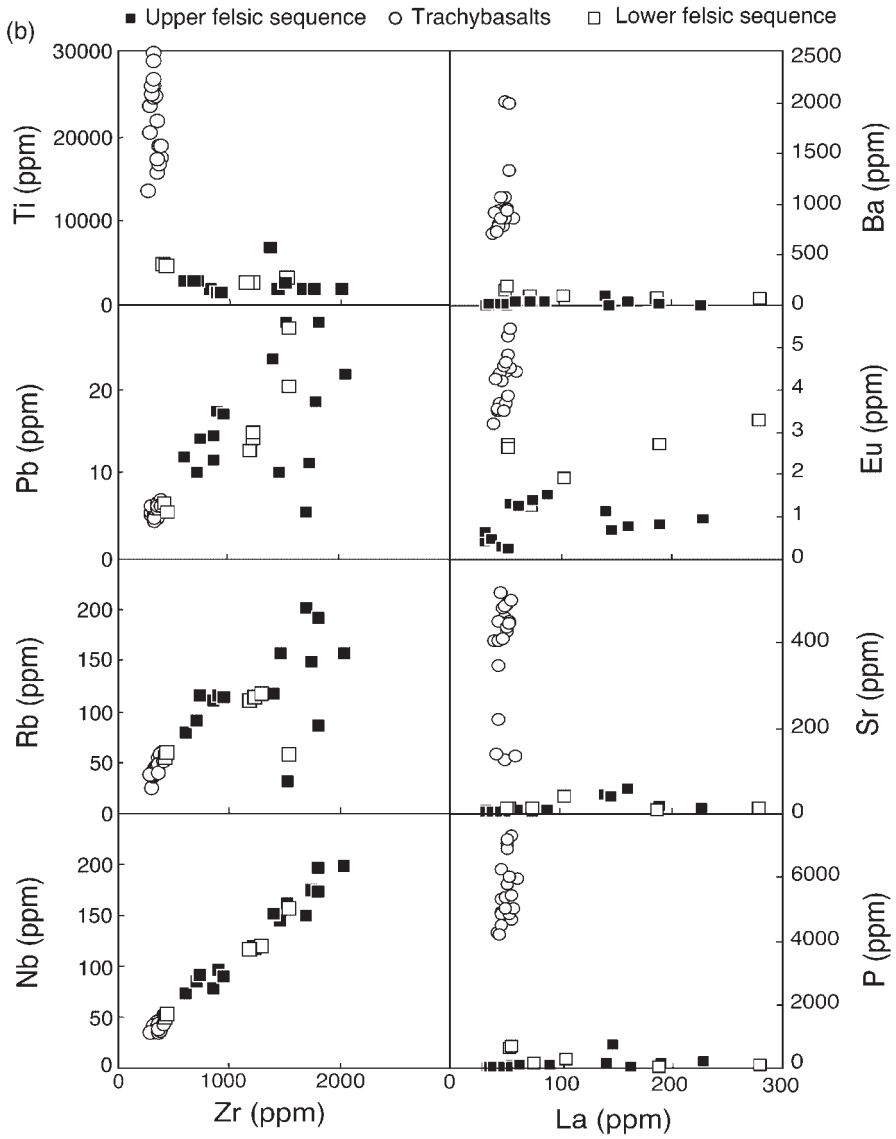

Fig. 8. Relationships between trace element concentrations and ratios. Noteworthy features are the good correlation between Zr and Th or Nb, the wide scatter for mobile elements such as Cs, U and Rb, and the contrasting trends in mafic and felsic rocks for elements involved in fractional crystallization (Ti, Sr, Ba, Eu, P).

indicate that the mantle source had an intermediate composition, neither strongly depleted nor enriched, like that of most samples from the southern and central plateau (Fig. 10). The transition from the relatively flat trace element patterns in the majority of Kerguelen Plateau basalts (Salters *et al.*, 1992) to the more enriched patterns in the Site 1139 lavas may indicate a change in the conditions of melting (an increase in the depth of melting associated with a fall in the temperature of the source) or a change in the composition of the source. We attempt to distinguish between these interpretations after discussion of the tectonic evolution of the northern part of the plateau.

Felsic volcanic rocks

We cannot learn a great deal about the magmatic processes that produce felsic volcanic rocks solely by studying two relatively thin sequences of highly altered rocks. Even in regions where bimodal volcanic sequences are well preserved and can be studied in outcrop, there is often no consensus as to whether the felsic rocks formed through fractional crystallization of basaltic parental magmas or by partial melting of mafic rocks (e.g. Bohrson & Reid, 1997; Trua *et al.*, 1999; Ayalew, 2000; Deniel *et al.*, 2000). In view of these complications, our approach has been first to attempt to distinguish between the effects of alteration and magmatic processes, then to compare the

Table 2: Measured and calculated initial isotopic ratios

Sample	Unit		$^{206}Pb/^{204}Pb$	$^{207}Pb/^{204}Pb$	$^{208}Pb/^{204}Pb$	$(^{87}Sr/^{86}Sr)_m$	Error (±)*	$(^{87}Sr/^{86}Sr)_i$	$(^{143}Nd/^{144}Nd)_m$	Error (±)*	$(^{143}Nd/^{144}Nd)_i$	$\varepsilon(Nd)_i$
51R1 13–19	1	Felsic	17·862	15·541	38·645				0·512594	5	0·51251	–0·76
51R1 13–19 duplicate	1	Felsic				1·015175	9	0·941638				
52R1 2–7	1	Felsic	17·711	15·524	38·655	1·442100	89	1·365246	0·512573	4	0·51249	–1·15
52R1 2–7 duplicate	1	Felsic	17·687	15·527	38·518	1·441548	74	1·364698	0·512545	3	0·51247	–1·70
52R1 2–7 not leached	1	Felsic				0·781033	5	0·711516	0·512543	4	0·51246	–1·73
52R1 2–7 leachate	1					0·710758	7					
54R1 1–9	1	Felsic	17·649	15·526	38·366	1·582557	32	1·495943	0·512530	5	0·51242	–2·50
54R1 1–9 not leached	1	Felsic				0·791156	6	0·713607	0·512554	3	0·51245	–2·04
54R1 1–9 leachate	1					0·719410	4		0·512540	5		
57R1127–134	4	Felsic	17·702	15·516	38·283				0·512544	5	0·51248	–1·32
57R1127–134 duplicate	4	Felsic	17·726	15·536	38·366				0·512535	4	0·51247	–1·50
57R1127–134 duplicate	4	Felsic	17·674	15·510	38·231	0·915856	7	0·813572				
57R1127–134 leachate	4					0·726904	4					
61R1 67–73	5	Felsic	17·902	15·542	38·407	0·775811	6	0·744190	0·512621	4	0·51257	0·31
61R2 93–97	5	Felsic	17·911	15·542	38·406	0·766991	6	0·730505	0·512586	5	0·51253	–0·34
62R2 74–79	6	Mafic	17·539	15·515	38·080	0·707145	4	0·705905	0·512514	6	0·51246	–1·82
64R1127–135	7	Mafic	17·501	15·501	38·041	0·705855	5	0·705538				
64R1 136–146	7	Mafic	17·507	15·497	38·035	0·705860	4	0·705542	0·512527	5	0·51247	–1·55
64R2 78–87	7	Mafic	17·505	15·503	38·041	0·705832	4	0·705464	0·512630	7	0·51257	0·47
64R2 78–87 duplicate	7	Mafic				0·705895	6	0·705527				
64R4 103–115	8	Mafic	17·579	15·519	38·095	0·705698	6	0·705446	0·512524	5	0·51247	–1·63
64R4 103–115 duplicate	8	Mafic	17·580	15·515	38·088	0·705693	5	0·705441	0·512541	6	0·51248	–1·30
65R3 15–19	10	Mafic	17·584	15·554	38·230	0·705930	5	0·705619	0·512523	7	0·51247	–1·65
65R3 15–19 duplicate	10	Mafic	17·556	15·524	38·128	0·705952	5	0·705641	0·512516	5	0·51246	–1·80
66R3 2–10	12	Mafic	17·599	15·543	38·190	0·705887	6	0·705654	0·512545	6	0·51249	–1·23
67R4 35–41	14	Mafic	17·566	15·517	38·107	0·706604	6	0·705841	0·512763	7	0·51271	3·02
69R2105–109	17	Mafic	17·537	15·501	38·054	0·705940	6	0·705616	0·512519	5	0·51246	–1·71
70R4 108–118	18	Felsic	17·683	15·544	38·282	0·721412	6	0·710687	0·512530	4	0·51247	–1·53
71R4 40–50	18	Felsic	17·610	15·514	38·215	0·710483	5	0·706378	0·512559	4	0·51250	–0·96
72R2 25–35	19	Felsic	17·769	15·545	38·496	0·760923	8	0·727382	0·512560	6	0·51251	–0·86
72R2 25–35 duplicate	19	Felsic	17·756	15·541	38·442							
73R3 100–111	19	Felsic	17·737	15·554	38·450							
73R3 100–111 duplicate	19	Felsic	17·702	15·518	38·342	0·742230	6	0·714962	0·512502	4	0·51245	–1·90

*Error on the sixth decimal place.

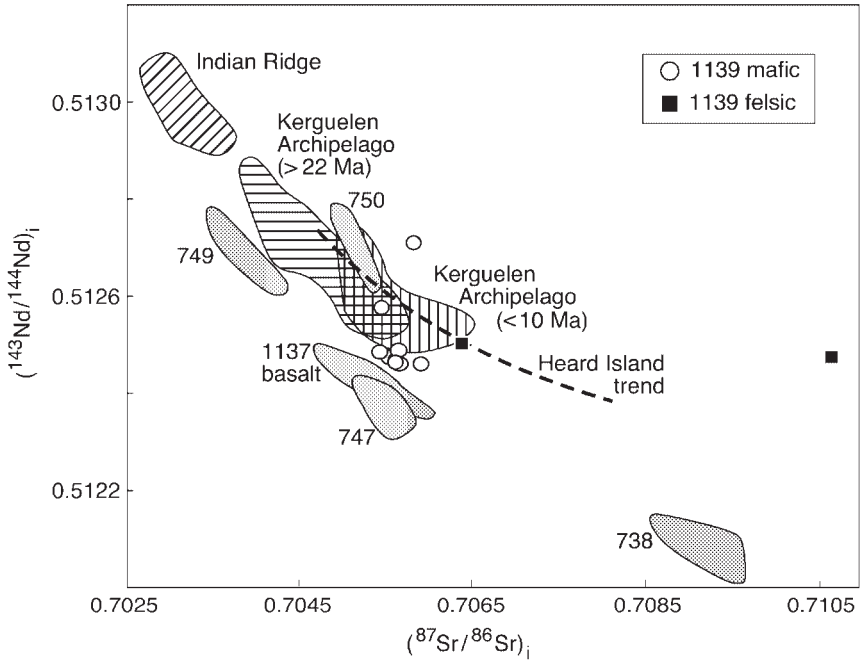

Fig. 9. $(^{87}Sr/^{86}Sr)_i$ vs $(^{143}Nd/^{144}Nd)_i$. Compositions are age corrected to 68 Ma using ICP-MS data. Most of the felsic samples have very high $^{87}Sr/^{86}Sr$ ratios and plot off scale. Fields representing rocks from other parts of the Kerguelen Plateau are from Salters *et al.* (1992), Mahoney *et al.* (1995) and Frey *et al.* (2002); those for the Archipelago are from Weis *et al.* (1993, 1998), Yang *et al.* (1998) and Frey *et al.* (2000*b*). The Heard Island trend is taken from Barling *et al.* (1994) and the field representing the Indian Ridge is from Mahoney *et al.* (1992) and Dosso *et al.* (1988).

compositions and characteristics of the Site 1139 rocks with those of well-preserved sequences from regions where the tectonic setting is better understood. In this way we can establish the significance of the petrological and chemical features preserved in the Site 1139 volcanic rocks and then use these features to determine the tectonic setting in which the rocks were erupted.

Recorded in the trace element patterns of the Site 1139 felsic lavas is evidence of two separate processes: low-pressure fractional crystallization, and alteration. The extremely low concentrations of certain elements pinpoint the role of the major fractionating minerals: Sr and Eu were extracted by plagioclase and K-feldspar; Ba by K-feldspar; P by apatite; and Ti by Fe–Ti oxides. In addition to these minerals, one or more ferromagnesian minerals must have fractionated to reduce the MgO and FeO contents. Because of the alteration we cannot use major elements to model this fractionation and instead have to rely on the trace elements. The procedure we adopted was to assume that the mantle-normalized pattern for the parental magma contained no anomalies. We then estimated the proportions of fractionating minerals, subtracting each mineral from the mafic composition until the anomalies in the felsic rocks are reproduced. The procedure depends strongly on the sets of partition coefficients adopted, but using standard values from Green's (1994) compilation, we calculated that the felsic rocks could have formed a parental trachybasaltic magma by 90% crystallization of an assemblage consisting of 10% clinopyroxene, 9% hornblende, 15% plagioclase, 51% K-feldspar, 7% apatite and 8% ilmenite (Fig. 13).

Because the REE, with the exception of Eu, are incompatible with feldspar, fractionation of plagioclase and K-feldspar will increase the concentrations of these elements. In contrast to their behaviour in mafic minerals, in feldspar the LREE are more compatible than the HREE (Arth, 1976). Magmas that evolve through feldspar fractionation therefore should have higher REE contents and flatter REE patterns than their parental magmas.

Qualitatively, the removal of feldspar provides an explanation for the relatively flat patterns of the three anomalous rhyolite samples from Unit 1 (51R1 13–19, 52R1 2–7 and 54R1 1–9; Fig. 7). These samples have extremely low contents not only of Sr and Eu but also of P and Ti, indicating that they underwent large amounts of fractional crystallization. Quantitatively, however, the explanation does not work. First, there is no correlation with modal mineralogy and major element compositions: samples with low REE contents and low La/Yb ratios include both high-Si rhyolites and (relatively) low-Si trachytes. Second, the changes in the concentrations and ratios of the REE are far greater than can be expected from feldspar fractionation alone. As shown in Fig. 13, extraction of 66% feldspar (the amount calculated from

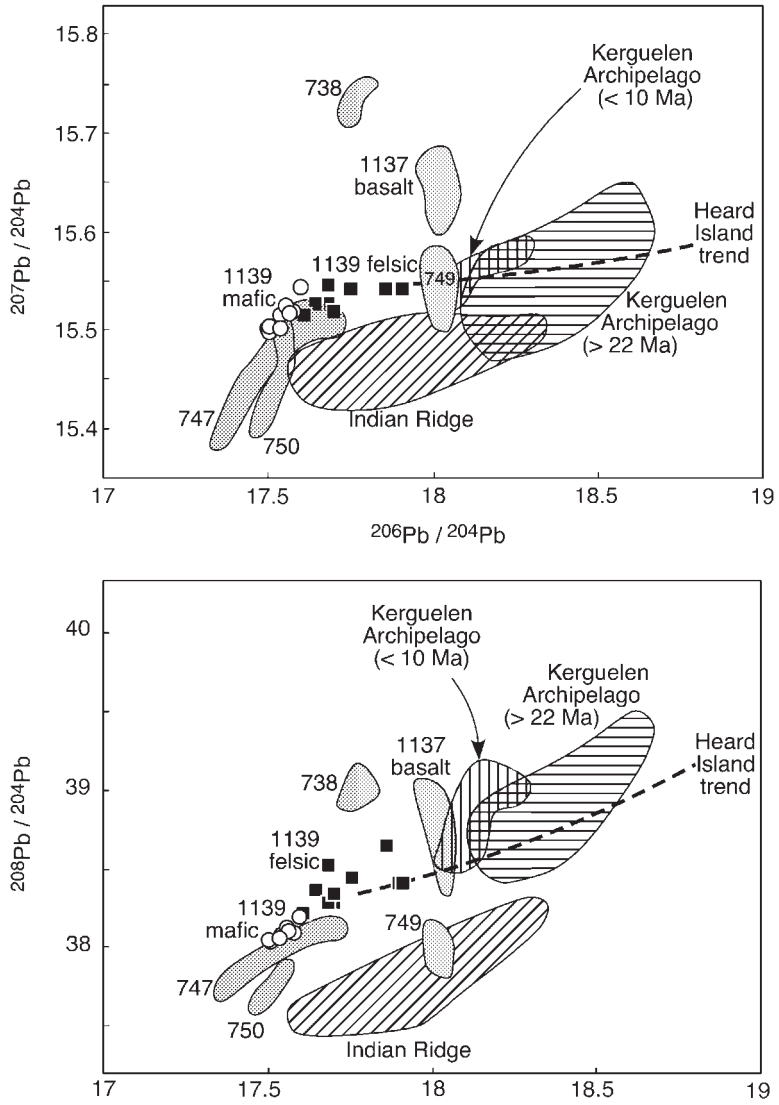

Fig. 10. Lead isotope diagrams. Data sources as in Fig. 9. Compositions are not age corrected.

Ba, Sr and Eu contents), as well as the minor phases listed above, can account for only a fraction of the variations of REE concentrations and ratios measured in the felsic rocks. These discrepancies could be taken as evidence either for mobility of the REE, or for independent derivation of the mafic and felsic lavas.

Sr and Pb isotopic compositions

As mentioned in an earlier section, both the measured and initial Pb isotopic ratios of the felsic lavas are slightly higher than in the mafic lavas. In view of the evidence of element mobility, how much significance can be placed on initial ratios calculated from U, Th and Pb contents of the whole rocks?

Three arguments suggest that the two groups of rocks could originally have had similar Pb isotopic composition and that the difference in measured isotopic composition is due to isotopic evolution: (1) the measured Pb isotope compositions, when viewed at the scale of variations throughout the entire Kerguelen Plateau, are not widely different in the two groups of rocks; (2) the U/Pb and Th/Pb ratios required if the felsic lavas were to evolve to their present position are 0·32 and 1·49, similar to those of the unaltered felsic lavas on the Kerguelen Archipelago ($\sim$0·3 and $\sim$1·35); (3) the initial Nd isotopic compositions of the felsic lavas are identical, within error, to those of the mafic lavas.

These parent–daughter ratios are significantly higher than those measured by ICP-MS on whole-rock samples.

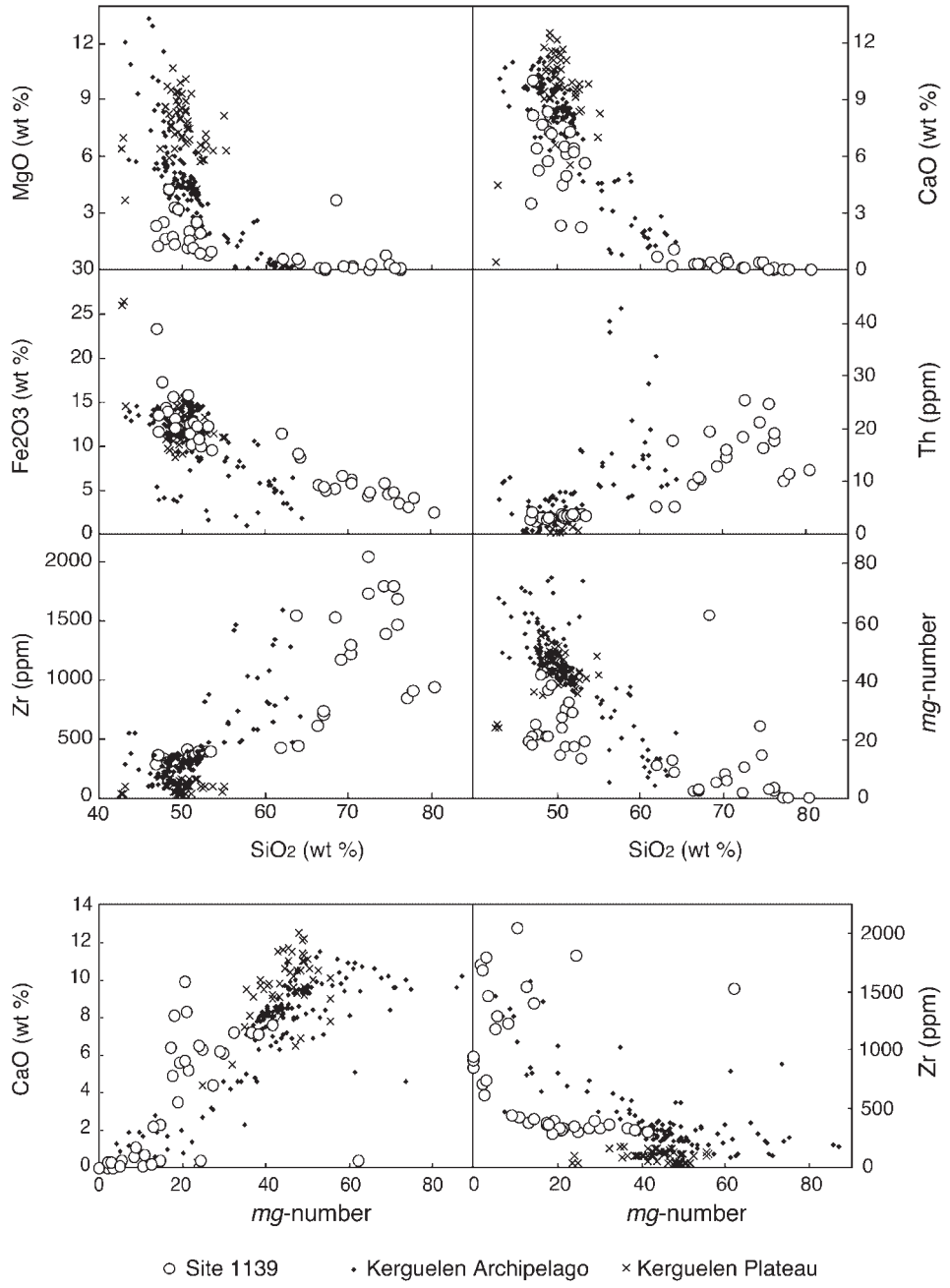

Fig. 11. Comparison of the major and trace element compositions of Site 1139 lavas with rocks from other parts of the plateau. Data are from Weis *et al.* (1993, 1998), Yang *et al.* (1998) and Frey *et al.* (2000*b*).

The Zr vs Pb diagram (Fig. 8b) shows that most samples fall on a moderately tight trend, but five samples have lower Pb contents. If these are excluded, the average ratios are U/Pb ~0·14 and Th/Pb ~0·83. To explain the difference between the required ratios and those actually measured in the samples, one solution is that the felsic rocks had gained Pb. However, unless the foreign Pb had the same composition as that of the samples, Pb gain would have changed the isotopic composition. Another possibility is that the samples lost U and Th, and that this loss was relatively recent. Although U is a mobile element, Th is assumed to be immobile, as is confirmed by its very good correlation with Zr (Fig. 8a). The measured Th/Pb ratio (0·83) is far from the calculated value of 1·49, which implies that the Pb isotopic composition of the felsic and mafic lavas may

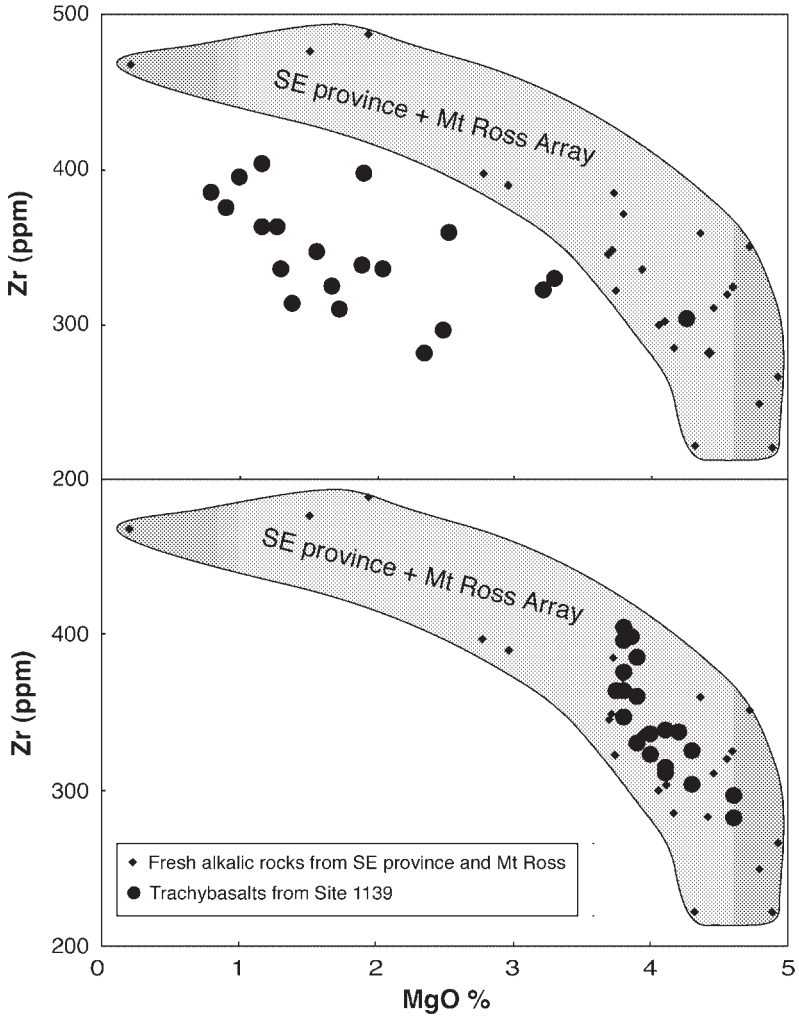

Fig. 12. Procedure used to correct the major element compositions of trachybasalts from Site 1139. The grey field represents the compositions of unaltered alkalic rocks from the Kerguelen Archipelago (from Weis *et al.*, 1993, 1998; Frey *et al.*, 2000*b*). A similar procedure was used to correct CaO and Fe_2O_3.

initially have been slightly different. The felsic magmas could perhaps have fractionated in crustal magma chambers where they interacted with slightly older, possibly altered surrounding rocks.

The high $^{87}Sr/^{86}Sr$ ratios measured in the leached felsic lavas probably result from preferential removal in the leachate of a component with a high Sr content and low Rb/Sr. The elimination of this component left a residue with high Rb/Sr that evolved to give high $^{87}Sr/^{86}Sr$. This hypothesis is confirmed by the low $^{87}Sr/^{86}Sr$ ratios of the leachates (0·7108 and 0·7194). Cousens *et al.* (1993) observed similar behaviour during their leaching experiments on felsic volcanic rocks from the Canary Islands. We did not measure Rb/Sr in the leached residue and cannot calculate reliable initial values. The mobility of REE elements casts some doubt on the validity of the initial Nd isotopic compositions of the felsic lavas. However, in this case their compositions fall within the same range as the mafic lavas, and the correction for isotopic decay over 68 Ma is relatively low.

What emerges from this discussion is the following. The trace element contents of the felsic volcanic rocks, and probably their Sr and Pb isotope compositions as well, were affected to some extent by alteration. The concentrations and the ratios of most trace elements, including the normally resistant REE, differ from those in the original magmas. For the HREE, the four-fold difference in concentrations (e.g. 4·3–18·5 ppm for Er) is at least in part a secondary effect. However, the overall form of the trace element patterns—their relatively flat slopes and large negative anomalies—is probably a true reflection of their original compositions. Furthermore,

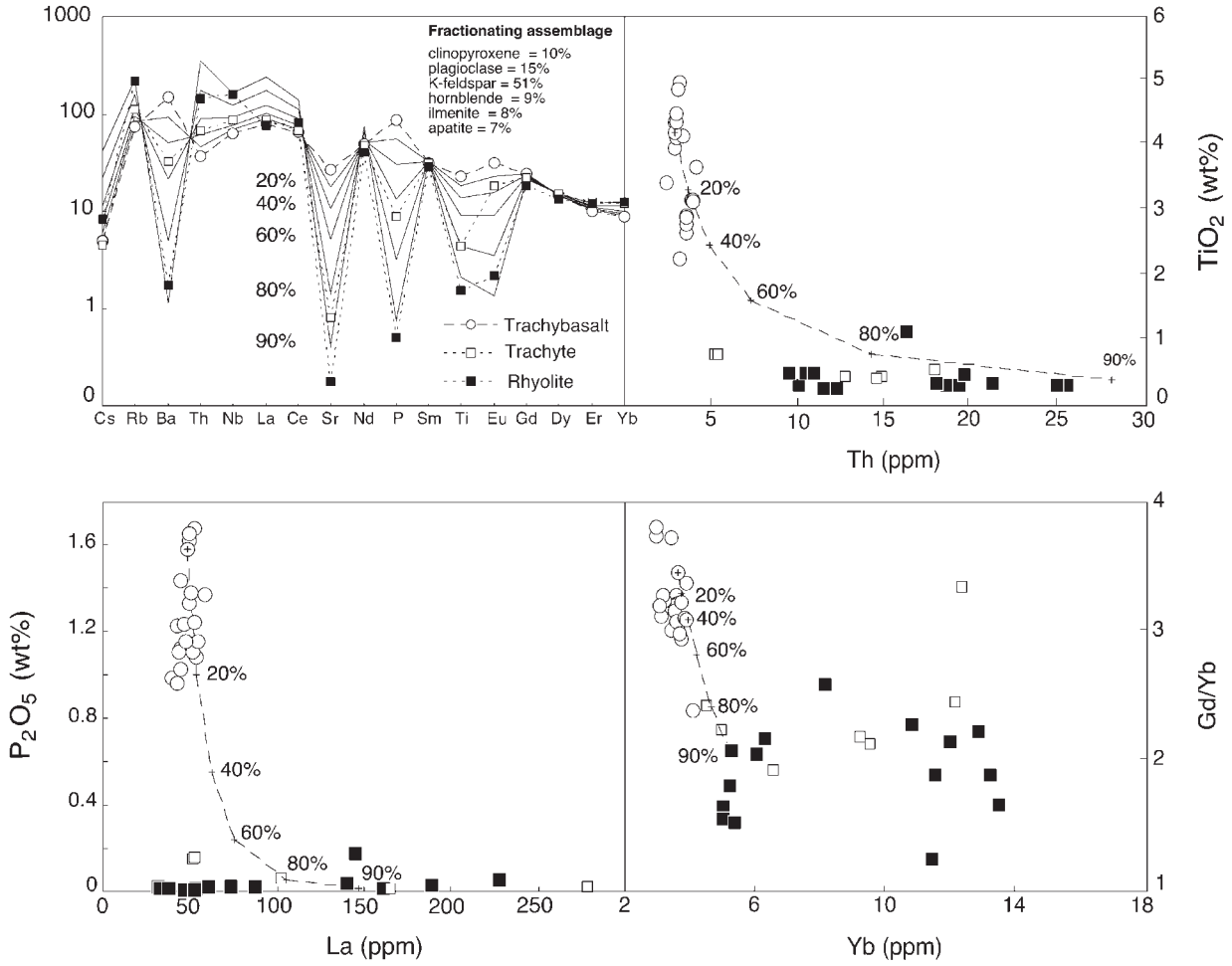

Fig. 13. Results of a model to simulate derivation of the felsic rocks from parental trachybasalt by crystal fractionation of clinopyroxene, plagioclase, K-feldspar, hornblende, ilmenite and apatite. The poor fit between the analytical data and the calculated trend implies that the felsic rocks were not derived from the trachybasalts by simple fractional crystallization.

the concentrations of a few elements, such as the HFSE and perhaps Th as well, may have been little affected by alteration.

In this light we cautiously interpret the varations in major and trace elements in Fig. 13 as evidence that the felsic volcanic rocks were not derived directly by fractional crystallization of the trachybasalts. In each of these diagrams, many of the felsic volcanic rocks plot well off the fractional crystallization trends. The concentrations of Th and La in many of the felsic rocks are similar to, or only slightly higher than those in the trachybasalts (Figs 7, 8 and 13). The fractional crystallization models, on the other hand, produce melts that have Th and La abundances up to five times higher than in the felsic lavas. Taken together with the possibility that the Pb isotope compositions of the two groups of rocks may have differed, these results suggest that the felsic magmas formed not by fractional crystallization but by partial melting of a mafic source. A series of melts with intermediate compositions and variable extents of silica saturation may have been produced, and these fractionally crystallized to form the trachytes and rhyolites. The flat HREE patterns indicate that the melting took place in the absence of garnet, which suggests melting at relatively shallow depths, perhaps near the base of the volcanic pile.

Nature and timing of the alteration

In the initial report of the Shipboard Scientific Party, the structures and textures of the volcanic rocks of Site 1139 were interpreted to indicate subaerial eruption. From the age dating of Duncan (2002), we know that the eruption took place 68–66 Ma ago. The age of the chalk of the sedimentary Unit III (Shipboard Scientific

Party, 2000), which lies ~80 m above the volcanic rocks, is ~34 Ma, but a sequence of shallow-water sedimentary rocks intervenes between this unit and the volcanic rocks. We infer, therefore, that the rocks remained subaerial for some unknown portion of the 32 Myr period between the eruption of the volcanic rocks and deposition of the chalk. The problem is to establish the timing and origin of the intense alteration that has affected the rocks. Unless the plateau foundered immediately after eruption of the Site 1139 volcanic rocks, the role of seawater is unlikely to be important.

It is most likely that the alteration resulted from processes within the subaerial volcanic pile. The nature of the secondary minerals in the intensely altered lower trachytic flows, particularly the presence of siderite, chalcedony and clay minerals in the matrix of these rocks, resembles those of rocks affected by the circulation of fluids derived from high-level alkalic intrusions (Vartiainen & Wooley, 1976).

Another possibility is that the rocks were affected by fumarolic activity or by weathering, which may have contributed to the removal of MgO and CaO and addition of FeO seen in the mafic lavas. For a better understanding of these processes we await the results of a parallel study of mineralogical aspects of the alteration of Site 1139 volcanic rocks, which is currently being undertaken by D. Teagle at the Southampton Oceanographic Institute.

Continental crust contamination

An important element in the interpretation of lavas from the Kerguelen Plateau is the extent to which they record interaction with continental lithosphere. The presence of a continental component in rocks from Sites 738 and 1137 (Mahoney *et al.*, 1995; Weis *et al.*, 2001; Ingle *et al.*, 2002) provides convincing arguments that basalts in several parts of the older southern plateau and Elan Bank erupted onto or near continental lithosphere, in the manner of continental flood basalts.

The volcanic rocks of Site 1139 show no convincing evidence of continental material. The trachybasalts have relatively low Nb/La ratios, which could be taken as an indication of a crustal component, but the same lavas also contain low concentrations of Th and U. In most rocks from the upper continental crust—granitoids, sediments and metamorphic rocks—mantle-normalized Th contents are far higher than mantle-normalized Nb contents (Rudnick, 1995). The signature of crust contamination is a negative Nb anomaly—low Nb/La accompanied by high Th/Nb. Some high-grade granulites are relatively depleted in Th, but this depletion normally is accompanied by far more pronounced depletion of elements such as Rb and U (Rudnick & Fountain, 1995). In the trachybasalts, Rb is undepleted. We are aware that these elements may be mobile and recognize the possibility that their concentrations could have been increased during the later alteration. However, the relative constancy, particularly of Th/Nb ratios, suggests that low Th is a primary feature. Negative Th and U anomalies have been recognized in several other suites of plume-related basalts, such as in non-contaminated members of the Coppermine and Ethiopian continental flood basalts (Griselin & Arndt, 1996; Pik *et al.*, 1999). In these series, the low Th and U contents are interpreted as a source feature of unknown origin.

The felsic volcanic rocks show a wide range of Nb/La ratios, which, as explained above, is the combined result of fractional crystallization and element mobility. If these rocks had once had low Nb/La, this feature has been masked by subsequent element mobility.

On balance, it seems that the volcanic rocks from Site 1139 have not interacted with continental lithosphere.

Tectonic setting

In an earlier section we compared the compositions of Site 1139 lavas with those of lavas from the rest of the plateau. Broadly speaking, the Site 1139 rocks can be distinguished from the tholeiitic flood basalts throughout the plateau by their bimodal, alkalic character and by their strong enrichment of incompatible trace elements. Their Pb isotopic compositions are similar to those of lavas from Kerguelen Plateau (Sites 747 and 750) but different from those from Sites 738 and 1137, which were affected by contamination with upper crust.

In terms of their petrological character and their trace element contents, the Site 1139 lavas are more like some of the younger volcanic rocks on the Kerguelen Archipelago. The two suites are distinguished, however, by the presence of high-Si quartz-phyric rhyolites at Site 1139 and by low $^{206}Pb/^{204}Pb$ ratios in the Site 1139 rocks. In addition, there are the previously mentioned differences in the degree of alteration, and in the ages of the two groups of rocks: the Site 1139 rocks were dated at 68 Ma whereas the volcanism on the Kerguelen Archipelago ranges in age from 30 Ma to virtually the present (Weis *et al.*, 1993, 1998; Nicolaysen, 2000).

How can we explain these differences, and what do they tell us about the tectonic setting in which the rocks of Site 1139 were emplaced? We answer this question by comparing the rocks from Site 1139 with bimodal volcanic suites from three other regions: the Kerguelen Archipelago, modern oceanic islands, and the Ethiopia volcanic plateau.

The Kerguelen Archipelago is composed dominantly of tholeiitic to transitional flood basalts, overlain by younger volcanic edifices, some of which contain alkalic,

mafic to felsic suites. These volcanic rocks differ in two significant ways from the Site 1139 assemblage: (1) instead of having a bimodal distribution, the volcanic rocks display a semi-continuous range of composition, from mafic to felsic; (2) the most evolved members have trachytic to phonolitic compositions, and quartz-phyric rhyolites, like those of the upper series at Site 1139, are absent (Weis *et al.*, 1993, 1998; Frey *et al.*, 2000*b*).

Bimodal volcanic suites are present in a few oceanic islands. The best-known example is Iceland, where rhyolites make up ~12% of a volcanic pile dominated by tholeiitic basalts (Sigurdson, 1977; Johannesson & Saemundsson, 1989; Marsh *et al.*, 1991). Alkalic rocks are restricted to shield volcanoes, but these also contain a continuous range of compositions from basalt or basanite to trachyte. The association of siliceous rhyolite with alkalic mafic rocks is uncommon or absent. On islands such as the Canaries, Galapagos and Socorro, bimodal alkalic suites are present, but on these islands the felsic lavas are trachytes or low-Si rhyolites. We know of no reports, in modern oceanic islands, of high-Si quartz-phyric lavas like those from the upper series at Site 1139 (e.g. Cousens, 1990; Cousens *et al.*, 1993; Bohrson & Reid, 1997; Civetta *et al.*, 1998).

Most of the Ethiopian plateau formed by flood volcanism during an ~1 Myr interval at 30 Ma (Mohr & Zanettin, 1988; Hofmann *et al.*, 1997). Although the volcanic sequence is dominated by tholeiitic basalts, abundant (up to 30%) rhyolitic lavas and pyroclastic rocks are also present. Constructed on the volcanic plateau are numerous large shield volcanoes. The oldest of these appear to be penecontemporaneous with the flood volcanic rocks; others have ages ranging down to ~10 Ma, some 20 Myr younger than the flood basalts. There appears to be a systematic relationship between the age and the petrological character of the shield volcanoes (Kieffer *et al.*, in preparation). The older (~30 Ma) volcanoes are composed dominantly of tholeiitic basalt; alkalic rocks, where present, are restricted to minor late-stage eruptions. The younger shields contain a higher proportion of alkalic lavas. They commonly are bimodal, containing mafic members of basaltic to phonolitic compositions and felsic members with both trachytic and quartz-phyric rhyolitic compositions. Although the volcanic plateau was constructed on continental lithosphere, only the older tholeiitic lavas show trace element and isotopic evidence of interaction with continental crust (Pik *et al.*, 1999). Such evidence is totally lacking in the bimodal volcanic series of the younger shield volcanoes.

In the light of this comparison, we suggest that the volcanic sequence at Site 1139 formed part of a shield volcano constructed on an older volcanic plateau. Only in such settings do we find bimodal sequences of alkalic mafic lavas and felsic rocks that contain both trachyte and rhyolite. If the analogy is correct, we have to accept that the underlying flood basalts may be significantly older than the 68 Ma eruption age of the Site 1139 rocks.

We have very few independent constraints on the age of the thick crustal sequence that underlies the volcanic rocks drilled at Site 1139. The time of eruption is bracketed by the 90 Ma age obtained from Site 1138 in the central plateau, ~800 km SE of Site 1139, ages around 94 Ma from Site 1142 on the eastern part of Broken Ridge (Pringle & Duncan, 2000; Duncan, 2002), and an age of 34 Ma from Site 1140 in the northern plateau (Duncan, 2002), ~500 km to the NE of Site 1139. A similar low age of 38 Ma was obtained from Site 254 on the southern end of Ninetyeast Ridge (Duncan, 1978). As summarized by Duncan (2002), and Coffin *et al.* (2002), the age of the plateau broadly decreases from the southern to central plateau, from 119 Ma to ~94 Ma, and ages younger than ~35 Ma are restricted to those parts of the plateau adjacent to the Southeast Indian Ridge, at the northernmost end of the Kerguelen Plateau and the western end of Broken Ridge. It can be concluded therefore that the bimodal volcanic series at Site 1139 erupted onto a volcanic plateau whose age was somewhere between 68 Ma and ~90 Ma.

It is in this context that questions concerning the magmatic and tectonic history of the plateau, and the past location of the 'Kerguelen hotspot', must be addressed. Skiff Bank certainly does not correspond to the present site of the hotspot, as proposed by Müller *et al.* (1993); the volcanism is far too old. This result corroborates the interpretation of Steinberger (2000) and Weis *et al.* (2002), who do not place the plume below Skiff Bank. Steinberger proposed a location below the Kerguelen Archipelago on the basis of plume advection in a realistic mantle flow field, whereas Weis *et al.* used age data and geochemical results to infer a plume track between Heard Island and the Archipelago. Nor can it be assumed that the hotspot was located at Site 1139 68 Myr ago, because, in Ethiopia, the distribution of shield volcanoes appears to be controlled by structural features and to be unrelated to the inferred site of the mantle plume.

The volcanic rocks of Site 1139, as well as the flood basalts at the neighbouring Sites 1137 and 1138, are thought to have erupted subaerially (Frey *et al.*, 2000*a*). It is likely, therefore, that the upper parts of the 14–19 km thick crust that underlies the bimodal volcanic rocks of Site 1139 also consists of subaerial volcanic rocks, at least in part. The nature of the lower part of the crust and lithosphere is uncertain. Unlike Site 1137 on Elan Bank, which is interpreted as a microcontinent on the basis of geophysical data (Charvis *et al.*, 1997; Borissova *et al.*, 2000) and where the volcanic rocks contain clear geological and geochemical evidence of interaction with continental material, there is no direct evidence for the

presence of continental material at Site 1139. At Site 1139, all that can be said is that the volcanic rocks were emplaced subaerially onto a thick volcanic platform.

How then do we explain the alkalic character of Site 1139 rocks? In several continental flood basalt provinces (e.g. Ethiopia, Merla *et al.*, 1979; Mohr & Zanettin, 1988; and Siberia, Arndt *et al.*, 1998), alkalic volcanic rocks erupted penecontemporaneously with tholeiitic basalts. The difference in magmatic character is best interpreted in terms of differences in the degree of melting of their mantle source. These differences are not readily attributable to differences in lithosphere thickness nor to variations in the composition of the mantle source (there is little difference in the isotopic compositions of the two types of magma). In these regions, tholeiitic volcanism, the product of high-degree melting, may continue to the end of the volcanic episode, to form the uppermost flows in kilometre-thick volcanic piles. This is also the case in most of the Sites on the southern and central Kerguelen Plateau. In other sections through the Siberian flood volcanic rocks, tholeiitic flows are intercalated with alkalic flows, indicating contemporaneous eruption. In each of these regions, the differences between alkalic and tholeiitic magmas appear to be related mainly to variations in the temperature of the source (Kieffer *et al.*, in preparation). If these arguments are correct, then the alkalic character of Site 1139 lavas indicates only that the parental magmas were derived from a cooler part of the source; the composition of these rocks provides little information about the structure of the lithosphere, nor about their tectonic setting.

CONCLUSIONS

(1) The volcanic basement at Site 1139 consists of a sequence of 73 m thickness of trachybasaltic lava flows between two sequences of felsic lavas and volcaniclastic rocks.

(2) All the volcanic rocks are moderately to highly altered. The mafic lavas appear to have lost MgO and CaO and in some cases gained FeO; the felsic lavas are characterized by mobility of a wide range of major and trace elements. Interpretation of the magmatic evolution of these rocks relies mainly on their petrographic characteristics and on a small range of immobile trace elements. These include the HFSE, Th and with some caveats, the REE.

(3) Despite these complications it appears that the entire sequence had an alkalic magmatic character, as indicated by high concentrations of alkalis and incompatible trace elements.

(4) Magmas parental to the trachybasalts formed through low degrees of melting of a relatively cool part of the mantle source. The felsic lavas formed independently, probably through partial melting of mafic rocks within the volcanic pile. Both types of magma then evolved through the fractional crystallization of mafic minerals, feldspar, Fe oxides and apatite.

(5) The volcanic sequence at Site 1139 probably formed part of a shield volcanic constructed $\sim$68 Myr ago on an older volcanic platform. The age and the nature of this platform are poorly constrained. It probably was erupted subaerially, at least in its upper portions, sometime between 68 and 90 Ma. We cannot totally exclude the presence of continental material in the crust onto which the underlying flood basalts erupted, but there is no evidence that any such material interacted with the lavas that were sampled at Site 1139.

ACKNOWLEDGEMENTS

This research used samples and data provided by the Ocean Drilling Program (ODP). The ODP is sponsored by the US National Science Foundation (NSF) and participating countries under management of Joint Oceanographic Institutions (JOI), inc. Funding for this research was provided by ODP France and the French CNRS. B.K. benefited from a Eurodoc fellowship. Claude Maerschalk, Stephanie Ingle, Francine Keller, Catherine Chauvel, Henriette Lapierre and Eric Lewin are thanked for help in the chemistry and mass spectrometric laboratories and for useful discussions. J. M. Rhodes of the University of Massachusetts provided major element analyses. The review comments of F. Frey, W. Bohrson and L. M. Larsen are greatly appreciated.

REFERENCES

Arndt, N. T., Chauvel, C., Fedorenko, V. & Czamanske, G. (1998). Two mantle sources, two plumbing systems: tholeiitic and alkaline magmatism of the Maymecha River basin, Siberian flood volcanic province. *Contributions to Mineralogy and Petrology* **133**, 297–313.

Arth, J. G. (1976). Behavior of trace elements during magmatic processes—a summary of theoretical models and their applications. *Journal of Research, US Geological Survey* **4**, 41–47.

Ayalew, D. (2000). Origin by fractional crustallization of transitional basalt for the Asela–Ziway pantellerites. Crustal control in the genesis of Plio-Quaternary bimodal magmatism of the Main Ethiopian Rift (MER): geochemical and isotopic (Sr, Nd, Pb) evidence, by Trua *et al.* 1999). *Chemical Geology* **168**, 1–3.

Barling, J., Goldstein, S. L. & Nicholls, I. A. (1994). Geochemistry of Heard Island (Southern Indian Ocean): characterization of an enriched mantle component and implications for enrichment of the sub-Indian Ocean mantle. *Journal of Petrology* **35**, 1017–1053.

Barrat, J. A., Keller, F., Amossé, J., Taylor, R. N., Nesbitt, R. W. & Hirata, T. (1996). Determination of rare earth elements in sixteen silicate reference samples by ICP-MS after Tm addition and ion exchange separation. *Geostandards Newsletter* **20**, 133–139.

Barrat, J. A., Blichert-Toft, J., Gillet, P. & Keller, F. (2000). The differentiation of eucrites: the role of *in situ* crystallization. *Meteoritics and Planetary Science* **35**, 1087–1100.

Bohrson, W. A. & Reid, M. R. (1997). Genesis of silicic peralkaline volcanic rocks in an ocean island setting by crustal melting and open-system processes: Socorro Island, Mexico. *Journal of Petrology* **38**, 1137–1166.

Borissova, I., Coffin, M. F., Moore, A., Sayers, J., Symonds, P. & Teliatnikov, I. (2000). Volcanostratigraphy of the Elan Bank (Kerguelen Plateau) and implication for the regional tectonics. *EOS Transactions, American Geophysical Union* **81**, S431.

Charvis, P., Recq, M., Operto, S. & Brefort, D. (1995). Deep structure of the northern Kerguelen Plateau and hotspot-related activity. *Geophysical Journal International* **122**, 899–924.

Charvis, P. Operto, S., Lesne, O. & Royer, J. Y. (1997). Velocity structure of the Kerguelen volcanic province from wide-angle seismic data: petrological implications. *EOS Transactions, American Geophysical Union* **78**, F711.

Civetta, L., D'Antonio, M., Orsi, G. & Tilton, G. R. (1998). The geochemistry of volcanic rocks from Pantelleria Island, Sicily Channel: petrogenesis and characteristics of the mantle source region. *Journal of Petrology* **39**, 1453–1491.

Coffin, M. F., Pringle, M. S., Duncan, R. A., Gladczenko, T. P., Storey, M., Müller, R. D. & Gahagan, L. A. (2002). Kerguelen hotspot magma output since 130 Ma. *Journal of Petrology* **43**, 1121–1139.

Cousens, B. L., Spera, F. J. & Tilton, G. R. (1990). Isotopic patterns in silicic ignimbrites and lava flows of the Mogan and lower Fataga Formations, Gran Canaria, Canary Islands: temporal changes in mantle source composition. *Earth and Planetary Science Letters* **96**, 319–335.

Cousens, B. L., Spera, F. J. & Dobson, P. F. (1993). Post-eruptive alteration of silicic ignimbrites and lavas, Gran Canaria, Canary Islands: strontium, neodymium, lead, and oxygen isotopic evidence. *Geochimica et Cosmochimica Acta* **57**, 631–640.

Deniel, C., Trua, T. & Mazzuoli, R. (2000). Crustal control in the genesis of Plio-Quaternary bimodal magmatism of the Main Ethiopian Rift: geochemical and isotopic (Sr, Nd, Pb) evidence—reply. *Chemical Geology* **168**, 5–7.

Dosso, L., Bougault, H., Beuzart, P., Calvez, J. Y. & Joron, J. L. (1988). The geochemical structure of the South-East Indian ridge. *Earth and Planetary Science Letters* **88**, 47–59.

Doucet, S., Weis, D., Scoates, J. S., Nicolaysen, K., Frey, F. A. & Giret, A. (2002). The depleted mantle component in Kerguelen Archipelago basalts: petrogenesis of tholeiitic–transitional basalts from the Loranchet Peninsula. *Journal of Petrology* **43**, 1341–1366.

Duncan, R. A. (1978). Geochronology of basalts from the Ninetyeast Ridge and continental dispersion in the Eastern Indian Ocean. *Journal of Volcanology and Geothermal Research* **4**, 283–305.

Duncan, R. A. (2002). A time frame for construction of the Kerguelen Plateau and Broken Ridge. *Journal of Petrology* **43**, 1109–1119.

Duncan, R. A. & Pringle, M. S. (2000). Basement ages from the northern Kerguelen Plateau and Broken Ridge. *EOS Transactions, American Geophysical Union* **81**(19), S424.

Duncan, R. A. & Storey, M. (1992). The life cycle of Indian Ocean hotspots. In: Duncan, R. A., Rea, D. K., Kidd, R. B., von Rad, U. & Weissel, J. K. (eds) *Synthesis of Results from Scientific Drilling in the Indian Ocean. Geophysical Monograph, American Geophysical Union* **70**, 91–103.

Eggins, S. M., Woodhead, J. D., Kinsley, L. P. J., Mortimer, G. E., Sylvester, P., McCulloch, M. T., Hergt, J. M. & Handler, M. R. (1997). A simple method for the precise determination of >40 trace elements in geological samples by ICPMS using enriched isotope internal standardisation. *Chemical Geology* **134**, 311–326.

Frey, F. A., Coffin, M. F., Wallace, P. G., Weis, D., Zhao, X. & Shipboard Scientific Party (2000*a*). Origin and evolution of a submarine large igneous province: the Kerguelen Plateau and Broken Ridge, southern Indian Ocean. *Earth and Planetary Science Letters* **176**, 73–89.

Frey, F. A., Weis, D., Yang, H. J., Nicolaysen, K., Leyrit, H. & Giret, A. (2000*b*). Temporal geochemical trends in Kerguelen Archipelago basalts: evidence for decreasing magma supply from the Kerguelen Plume. *Chemical Geology* **164**, 61–80.

Frey, F. A., Weis, D., Borisova, A. Yu. & Xu, G. (2002). Involvement of continental crust in the formation of the Cretaceous Kerguelen Plateau: new perspectives from ODP Leg 120 sites. *Journal of Petrology* **43**, 1207–1239.

Gautier, I., Weis, D., Mennessier, J.-P., Vidal, P., Giret, A. & Loubet, M. (1990). Petrology and geochemistry of Kerguelen basalts (South Indian Ocean): evolution of the mantle sources from ridge to an intraplate position. *Earth and Planetary Science Letters* **100**, 59–76.

Green, T. H. (1994). Experimental studies of trace element partitioning applicable to igneous petrogenesis—Sedona 16 years later. *Chemical Geology* **117**, 1–36.

Griselin, M. & Arndt, N. T. (1996). Plume–lithosphere interaction and crustal contamination during formation of Coppermine River basalts, Northwest Territories, Canada. *Canadian Journal of Earth Sciences* **3**, 958–975.

Hofmann, A. W. (1988). Chemical differentiation of the Earth: the relationship between mantle, continental crust, and oceanic crust. *Earth and Planetary Science Letters* **90**, 297–314.

Hofmann, C., Courtillot, V., Feraud, G., Rochette, P., Yirgu, G., Ketefo, E. & Pik, R. (1997). Timing of the Ethiopian flood basalt event and implications for plume birth and global change. *Nature* **389**, 338–341.

Ingle, S., Weis, D., Scoates, J. S. & Frey, F. A. (2002). Relationship between the early Kerguelen plume and continental flood basalts of the paleo-Eastern Gondwanan margins. *Earth and Planetary Sciences* **197**, 35–50.

Johannesson, H. & Saemundsson, K. (1989). *Geological map of Iceland. 1:500 000. Bedrock geology*, 1st edn. Reykjavik: Icelandic Museum of Natural History and Icelandic Geological Survey.

Kuno, H. (1966). Lateral variation of basalt magma types across continental margins and island arcs. *Bulletin of Volcanology* **29**, 195–222.

Le Bas, M. J., Le Maître, R. W., Streickeisen, A. & Zanettin, B. (1986). A chemical classification of volcanic rocks based on the total alkali–silica diagram. *Journal of Petrology* **27**, 745–750.

Mahoney, J., Le Roex, A. P., Peng, Z., Fisher, R. L. & Natland, J. H. (1992). Southwestern limits of Indian Ocean ridge mantle and the origin of low $^{206}Pb/^{204}Pb$ mid-ocean ridge basalt: isotope systematics of the central southwest Indian ridge (17°–50°E). *Journal of Geophyical Research* **97**, 19771–19790.

Mahoney, J. J., Jones, W. B., Frey, F. A., Salters, V. J. M., Pyle, D. G. & Davies, H. L. (1995). Geochemical characteristics of lavas from Broken Ridge, the Naturaliste Plateau and southernmost Kerguelen plateau: Cretaceous plateau volcanism in the southeast Indian Ocean. *Chemical Geology* **120**, 315–345.

Marsh, B. D., Gunnarsson, B., Congdon, R. & Carmody, R. (1991). Hawaiian basalt and Icelandic rhyolite: indicators of differentiation and partial melting. *Geologische Rundschau* **80**, 481–510.

Merla, G., Abbate, E., Canuti, P., Sagri, M. & Tacconi, P. (1979). *Geological map of Ethiopia and Somalia and comment with a map of major landforms (scale 1:2 000 000)*. Rome: Consiglio Nazionale de la Ricerche.

Mohr, P. & Zanettin, B. (1988). The Ethiopian flood basalt province. In: MacDougall, J. D. (ed.) *Continental Flood Basalts*. Dordrecht: Kluwer Academic, pp. 63–110.

Müller, R. D., Royer, J. Y. & Lawver, L. A. (1993). Revised plate motions relative to the hotspots from combined Atlantic and Indian Ocean hotspot tracks. *Geology* **21**, 275–278.

Nicolaysen, K., Frey, F. A., Hodges, K. V., Weis, D. & Giret, A. (2000). 40Ar/39Ar geochronology of flood basalts from the Kerguelen Archipelago, southern Indian Ocean: implications for Cenozoic eruption rates of the Kerguelen plume. *Earth and Planetary Science Letters* **174**, 313–328.

Pik, R., Deniel, C., Coulon, C., Yirgu, G. & Marty, B. (1999). Isotopic and trace element signatures of Ethiopian basalts: evidence for plume–lithospheric interactions. *Geochimica et Cosmochimica Acta* **63**, 2263–2279.

Pringle, M. S. & Duncan, R. A. (2000). Basement ages from the southern and central Kerguelen Plateau: initial products of the Kerguelen Large Igneous Province. *EOS Transactions, American Geophysical Union* **81**(19), S424.

Recq, M. & Charvis, P. (1986). A seismic refraction survey in the Kerguelen Isles, southern Indian Ocean. *Geophysical Journal of the Royal Astronomical Society* **84**, 529–559.

Recq, M., Brefort, D., Malod, J. & Veinante, J.-L. (1990). The Kerguelen Isles (southern Indian Ocean); new results on deep structure from refraction profiles. *Tectonophysics* **182**, 227–248.

Recq, M., Operto, S. & Charvis, P. (1994). Kerguelen Plateau: a hotspot related oceanic crust. *EOS Transactions, American Geophysical Union* **75**, 583.

Rhodes, J. M. (1983). Homogeneity of lava flows: chemical data for historical Mauna Loa eruptions. *Journal of Geophysical Research, Supplement* **88**, A869–A879.

Rudnick, R. L. (1995). Making continental crust. *Nature* **378**, 571–577.

Rudnick, R. L. & Fountain, D. M. (1995). Nature and composition of the continental crust: a lower crustal perspective. *Reviews of Geophysics* **33**, 267–309.

Salters, V. J. M., Storey, M., Sevigny, J. H. & Whitechurch, H. (1992). Trace element and isotopic characteristics of Kerguelen–Heard plateau basalts. In: Wise, S. W., Jr & Schlich, R. (eds) *Proceedings of the Ocean Drilling Program, Scientific Results*, 120. College Station, TX: Ocean Drilling Program, pp. 55–62.

Sandwell, D. T. & Smith, W. H. F. (1997). Marine gravity anomaly from Geosat and ERS-1 satellite altimetry. *Journal of Geophysical Research* **102**, 10039–10054.

Schlich, R., Schaming, M., Weis, D., Montigny, R. & Damasceno, D. (1998). New structural and tectonic data in the Northern Kerguelen Plateau. *EOS Transactions, American Geophysical Union* **79**, F871.

Shipboard Scientific Party (2000). Leg 183 summary: Kerguelen Plateau–Broken Ridge. A large igneous province. In: Coffin, M. F., Frey, F. A. & Wallace, P. J. (eds) *Proceedings of the Ocean Drilling Program, Initial Reports*, 183. College Station, TX: Ocean Drilling Program, pp. 1–101.

Sigurdson, H. (1977). Generation of Icelandic rhyolites by melting of plagiogranites in the oceanic layer. *Nature* **269**, 25–28.

Steinberger, B. (2000). Plumes in a convecting mantle: models and observations for individual hotspots. *Journal of Geophysical Research* **105**, 11127–11152.

Storey, M., Kent, R., Saunders, A. D., Salters, V. J., Hergt, J., Whitechurch, H., Sevigny, J. H., Thirlwall, M. F., Leat, P., Ghose, N. C. & Gifford, M. (1992). Lower Cretaceous volcanic rocks along continental margins and their relationship to the Kerguelen Plateau. In: Wise, S. W., Jr & Schlich, R. (eds) *Proceedings of the Ocean Drilling Program, Scientific Results*, 120. College Station, TX: Ocean Drilling Program, pp. 33–53.

Sun, S.-S. & McDonough, W. F. (1989). Chemical and isotopic systematics of oceanic basalts: implications for mantle composition and processes. In: Saunders, A. D. & Norry, M. J. (eds) *Magmatism in the Ocean Basins. Geological Society, London, Special Publications* **42**, 313–345.

Trua, T., Deniel, C. & Mazzuoli, R. (1999). Crustal control in the genesis of Plio-Quaternary bimodal magmatism of the Main Ethiopian Rift (MER): geochemical and isotopic (Sr, Nd, Pb) evidence. *Chemical Geology* **155**, 201–231.

Vartiainen, H. & Wooley, A. R. (1976). The petrography, mineralogy and chemistry of the fenites of the Sokli carbonatite intrusion, Finland. *Geological Survey of Finland Bulletin*, **280**.

Weis, D. & Frey, F. A. (1991). Isotope geochemistry of Ninetyeast Ridge basalts: Sr, Nd, and Pb evidence for the involvement of the Kerguelen hot spot. In: Weissel, J., Peirce J., Taylor, E., Alt, J., *et al.* (eds) *Proceedings of the Ocean Drilling Program, Scientific Results*, 121. College Station, TX: Ocean Drilling Progam, pp. 591–610.

Weis, D. & Frey, F. A. (2002). Submarine basalts of the Northern Kerguelen Plateau: interaction between the Kerguelen plume and the Southeast Indian Ridge revealed at ODP Site 1140. *Journal of Petrology* **43**, 1287–1309.

Weis, D., Demaiffe, D., Cauët, S. & Javoy, M. (1987). Sr, Nd, O and H isotopic ratios in Ascension Island lavas and plutonic inclusions: cogenetic origin. *Earth and Planetary Science Letters* **82**, 255–268.

Weis, D., Frey, F. A., Leyrit, H. & Gautier, I. (1993). Kerguelen Archipelago revisited: geochemical and isotopic study of the SE Province lavas. *Earth and Planetary Science Letters* **118**, 101–119.

Weis, D., Frey, F. A., Giret, A. & Cantagrel, J. M. (1998). Geochemical characteristics of the youngest volcano (Mount Ross) in the Kerguelen Archipelago: inferences for magma flux and composition of the Kerguelen Plume. *Journal of Petrology* **39**, 973–994.

Weis, D., Ingle, S., Damasceno, D., Frey, F. A., Nicolaysen, K. & Barling, J. (2001). Origin of continental components in Indian Ocean basalt: Evidence from Elan Bank (Kerguelen Plateau, ODP Leg 183, Site 1137). *Geology* **29**, 147–150.

Weis, D., Frey, F. A., Schlich, R., Schaming, M., Montigny, R., Damasceno, D., Mattielli, N., Nicolaysen, K. E. & Scoates, J. S. (2002). Trace of the Kerguelen mantle plume: evidence from seamounts between the Kerguelen Archipelago and Heard Island, Indian Ocean. *G-Cubed—Geology, Geochemistry & Geophysics*, in press.

Yang, Y. J., Frey, F. A., Nicolaysen, K., Weis, D. & Giret, A. (1998). Petrogenesis of flood basalts forming the Northern Kerguelen Archipelago: implications for the Kerguelen Plume. *Journal of Petrology* **39**, 711–748.